

Contents lists available at [ScienceDirect](https://www.sciencedirect.com)

Environmental Research

journal homepage: www.elsevier.com/locate/envres

Review article



Exploring the nexus of urban form, transport, environment and health in large-scale urban studies: A state-of-the-art scoping review

Georgia M.C. Dyer^{a,b,c}, Sasha Khomenko^{a,b,c}, Deepti Adlakha^d, Susan Anenberg^e, Martin Behnisch^f, Geoff Boeing^g, Manuel Esperon-Rodriguez^{h,i}, Antonio Gasparrini^j, Haneen Khreis^k, Michelle C. Kondo^l, Pierre Masselot^j, Robert I. McDonald^m, Federica Montana^{a,b,c}, Rich Mitchellⁿ, Natalie Mueller^{a,b,c}, M. Omar Nawaz^e, Enrico Pisoni^o, Rafael Prieto-Curiel^p, Nazanin Rezaei^q, Hannes Taubenböck^{r,s}, Cathryn Tonne^{a,b,c}, Daniel Velázquez-Cortés^{a,b,c}, Mark Nieuwenhuijsen^{a,b,c,*}

^a Barcelona Institute for Global Health (ISGlobal), Doctor Aiguader 88, 08003, Barcelona, Spain^b Universitat Pompeu Fabra (UPF), Doctor Aiguader 88, 08003, Barcelona, Spain^c CIBER Epidemiología y Salud Pública (CIBERESP), Melchor Fernández Almagro, 3-5, 28029, Madrid, Spain^d Delft University of Technology, Mekelweg 5, 2628, Delft, Netherlands^e Environmental and Occupational Health Department, George Washington University, Milken Institute School of Public Health, 20052, New Hampshire Avenue, Washington, District of Columbia, United States^f Leibniz Institute of Ecological Urban and Regional Development, Weberpl 1, 01217, Dresden, Germany^g University of Southern California, 90007, Los Angeles, United States^h Hawkesbury Institute for the Environment, Western Sydney University, Locked Bag 1797, Penrith, NSW, 2751, Australiaⁱ School of Science, Western Sydney University, Locked Bag 1797, Penrith, NSW, 2751, Australia^j Environment & Health Modelling (EHM) Lab, Department of Public Health Environments and Society, London School of Hygiene & Tropical Medicine, 15-17 Tavistock Place, WC1E 7HT, London, United Kingdom^k MRC Epidemiology Unit, Cambridge University, CB2 0AH, Cambridge, United Kingdom^l USDA-Forest Service, Northern Research Station, 100 North 20th Street, Ste 205, 19103, Philadelphia, PA, United States^m The Nature Conservancy, 4245 North Fairfax Drive Arlington, 22203, Virginia, United Statesⁿ Institute of Health and Wellbeing, University of Glasgow, 90 Byres Road, Glasgow, G20 0TY, United Kingdom^o European Commission, Joint Research Centre (JRC), 2749, Ispra, Italy^p Complexity Science Hub Vienna, Josefstädter Straße 39, 1080, Vienna, Austria^q University of California Santa Cruz, 1156 High Street, 95064, California, United States^r German Aerospace Centre (DLR), Earth Observation Center (EOC), 82234, Oberpfaffenhofen, Germany^s Institute for Geography and Geology, Julius-Maximilians-Universität Würzburg, 97074, Würzburg, Germany

A B S T R A C T

Background: As the world becomes increasingly urbanised, there is recognition that public and planetary health relies upon a ubiquitous transition to sustainable cities. Disentanglement of the complex pathways of urban design, environmental exposures, and health, and the magnitude of these associations, remains a challenge. A state-of-the-art account of large-scale urban health studies is required to shape future research priorities and equity- and evidence-informed policies.

Objectives: The purpose of this review was to synthesise evidence from large-scale urban studies focused on the interaction between urban form, transport, environmental exposures, and health. This review sought to determine common methodologies applied, limitations, and future opportunities for improved research practice.

Methods: Based on a literature search, 2958 articles were reviewed that covered three themes of: urban form; urban environmental health; and urban indicators. Studies were prioritised for inclusion that analysed at least 90 cities to ensure broad geographic representation and generalisability. Of the initially identified studies, following expert consultation and exclusion criteria, 66 were included.

Results: The complexity of the urban ecosystem on health was evidenced from the context dependent effects of urban form variables on environmental exposures and health. Compact city designs were generally advantageous for reducing harmful environmental exposure and promoting health, with some exceptions. Methodological heterogeneity was indicative of key urban research challenges; notable limitations included exposure and health data at varied spatial scales and resolutions, limited availability of local-level sociodemographic data, and the lack of consensus on robust methodologies that encompass best research practice.

* Corresponding author. Barcelona Institute for Global Health (ISGlobal), Doctor Aiguader 88, 08003, Barcelona, Universitat Pompeu Fabra (UPF), CIBER, Spain.
E-mail address: mark.nieuwenhuijsen@isglobal.org (M. Nieuwenhuijsen).

<https://doi.org/10.1016/j.envres.2024.119324>

Received 25 March 2024; Received in revised form 30 May 2024; Accepted 31 May 2024

Available online 4 June 2024

0013-9351/© 2024 The Author(s). Published by Elsevier Inc. This is an open access article under the CC BY-NC-ND license (<http://creativecommons.org/licenses/by-nc-nd/4.0/>).

Conclusion: Future urban environmental health research for evidence-informed urban planning and policies requires a multi-faceted approach. Advances in geospatial and AI-driven techniques and urban indicators offer promising developments; however, there remains a wider call for increased data availability at local-levels, transparent and robust methodologies of large-scale urban studies, and greater exploration of urban health vulnerabilities and inequities.

1. Introduction

Currently, almost 60% of the global population (~4.8 billion people) live in the urban environment and by 2050 nearly seven out of ten people will inhabit cities (The World Bank. United Nations Population Division; The World Bank). There are a host of reasons attributed to the rising trend of migration and urbanisation; mainly, cities provide rich opportunities for education, employment, wealth, and innovation (Lenzi, 2019; Sarkar and Webster, 2017). Yet cities can also be a concentrated source of environmental exposure stressors (e.g., air pollution, noise, and heat) (Khomenko et al., 2021, 2022; Glazener et al., 2021a), perpetuate unhealthy lifestyles (Nieuwenhuijsen, 2020), and exacerbate health inequities (Giles-Corti et al., 2022). Concurrent with rapid urbanisation, climate change poses an additional threat to urban health and sustainability challenges (Anderson et al., 2022; Fagliano and Roux, 2018). Cities account for 75% of the world's energy-related greenhouse gas emissions (Ritchie, 2023) and can be a major contributor to biodiversity loss (Oke et al., 2021). Although viewed as the principal drivers of climate change, cities also offer a large part of the solution (UN General Assembly, 2015; Tonne et al., 2021). In Europe, initiatives that aim to reduce greenhouse gas emissions and achieve carbon neutrality include the EU's Green Deal (European Commission) and the Paris Climate Agreement (United Nations). These initiatives recognise the pivotal role of sustainable and liveable cities for achieving these objectives, which in turn will protect public and planetary health.

The pathways of urban form, environmental exposures, and health are intricate, and the magnitude of these associations have not been widely substantiated (Nieuwenhuijsen, 2016). Although cities are a complex system, a conceptual framework developed by Nieuwenhuijsen & Khreis (Nieuwenhuijsen and Khreis, 2016) (Fig. 1) illustrates the multitude of urban and transport planning pathways that contributes toward the health of urban populations. Urban form denotes the structure, design, and physical features of an urban environment (Eldesoky and Abdeldayem, 2023), captured by the urban design pillar in Fig. 1.

There are two dominant urban forms; the first, known as compact cities, is characterised by dense housing and road infrastructure, and the second by dispersed low density infrastructure with high sprawl (Nieuwenhuijsen, 2020; Behnisch et al., 2022). Both are notionally inconducive to health and sustainability, as the first lends itself to increased pollutant emissions and noise levels, accentuated hot temperatures, and reduced green space (Nieuwenhuijsen, 2020); whilst the second favours motorised traffic and motor vehicle dependency, poorer public transportation infrastructure, lower social cohesion, and reduced physical activity levels (Sarkar and Webster, 2017; Guthold et al., 2018). However, the compact city model has the conceptual benefits of shorter commuting distances that promote active mobility and increase social cohesion, which highlights the potential trade-offs and complexity of urban design (Bibri et al., 2020). Naturally, cities can be a combination of these forms.

The health burden attributable to environmental exposures in urban settings is well documented (Glazener et al., 2021a; Nieuwenhuijsen, 2020; Mueller et al., 2018). In 2019, particulate matter diameter 2.5 μm (PM_{2.5}) and ozone air pollution were estimated to cause 4.51 million premature deaths worldwide (Institute for Health Metrics and Evaluation's Global Burden of Disease and Institute HE, 2020), and road traffic injuries were ranked the leading cause of disability-adjusted life years (DALYs) for ages 10–49 years, ranking 10th for ages 50–74 years (Abbafati et al., 2020). Trends of increasing heat-related morbidity and mortality are largely ascribed to climate change (World Health Organisation, 2023) and are exacerbated in urban environments due to the urban heat island (UHI) effect, an occurrence wherein urban areas exhibit elevated temperatures compared to their rural surroundings (Deilami et al., 2018). In addition to premature mortality, heat-related impacts include increased mental health distress (Thompson et al., 2018), cardiorespiratory-mortality (Cheng et al., 2019), and hospital admissions (Wondmagegn et al., 2021). Although a lesser studied environmental risk factor, chronic exposure to noise pollution can also have adverse health effects; at least 20% of the European urban

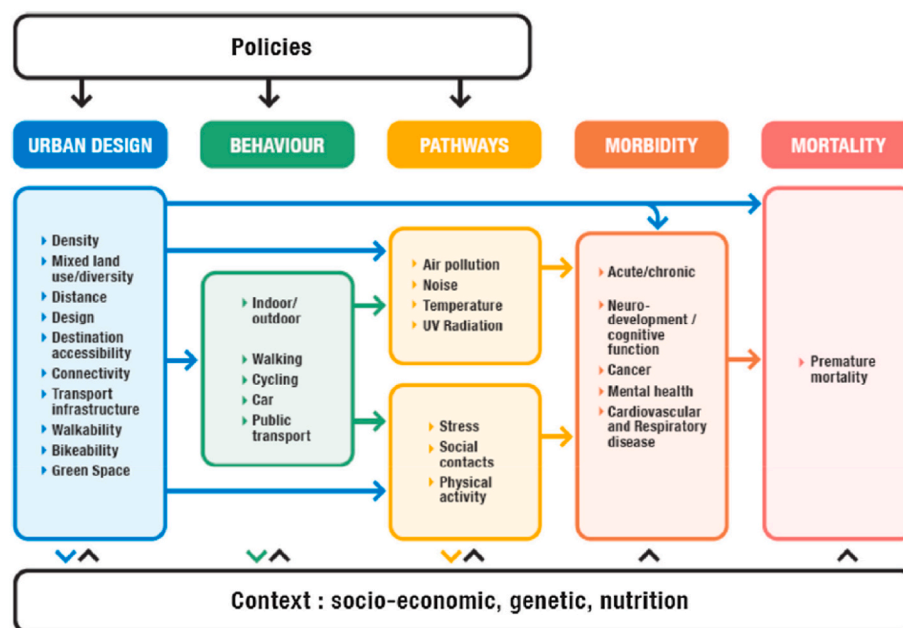


Fig. 1. Conceptual framework of the links and pathways between urban design, environmental exposures and health (Nieuwenhuijsen and Khreis, 2016).

population is likely to be exposed to noise levels harmful to health (European Environment Agency, 2023). In 2017, 18 million people in Europe were estimated to experience high annoyance from noise and 5 million sleep disturbance. Sedentary behaviour and reduced physical activity are well established risk factors of health burden and are often more prevalent in urban environments owing to lifestyles and built environment characteristics (Guthold et al., 2018). Perhaps the starkest of adverse impacts from sedentary behaviour (Park et al., 2020), sitting for 10 h a day is associated with 48% increased risk of all-cause mortality compared to 7.5 h a day (Henson et al., 2023).

Translating health burden statistics into actionable recommendations for policy requires research to effectively discern the intricate relation between urban form, environmental stressors, and health. However, uncovering causal inferences is complex due to the multiple pathways, long causal chains, and dynamic nature of contextual factors (e.g., neighbourhood attributes) and compositional (e.g., demographic characteristics) (Giles-Corti et al., 2016), alongside the multidisciplinary nature of urban and transport planning related impacts. Health impact assessment (HIA) is a widely adopted decision support tool that aids evidence-informed policies. HIAs are valuable within urban health research as the impacts of urban planning on health determinants and scenarios can be modelled and estimated impacts often have high comprehensibility to decision-makers, which helps generate awareness (Joffe and Mindell, 2005; Wismar et al., 2007). Temporal HIAs offer the additional advantage that predicted impacts reflect the historical trajectory of exposures and health burden, and thus, changes in exposure, impacts, and policies can be tracked over time (Mueller et al., 2023). To effectively interpret the accuracy of forecasted impacts and the existing evidence base necessitates understanding the uncertainties inherent in model assumptions and how these vary across studies (Mueller et al., 2023). Moreover, qualitative data, such as societal preferences, are integral in elucidating the constituents of an urban ecosystem. The Neighbourhood Environment Walkability Scale (NEWS) is one such tool designed to gather perceptions of neighbourhood attributes linked to physical activity (e.g., street connectivity) (Almeida et al., 2021). The widespread adoption of NEWS underscores the need for comprehensive, proxy tools that assess city liveability (Cerin et al., 2013). However there exists a plethora of different, context-specific walkability indices (Shank and Schuurman, 2019; Stockton et al., 2016; Puttaswamy et al., 2023; Carson et al., 2023); this underscores the resultant limitations in comparing studies that employ diverse methodologies, and the challenge in obtaining universally applicable insights into urban environmental health pathways and attributable impacts.

Large-scale urban studies offer generalisable and robust evidence for elucidating the nexus among city form, climate, transport, and environmental and health impacts. However, to the best of knowledge, there is no scoping review that synthesises evidence from large-scale urban studies that investigate these interconnections. Exploration of commonly employed methodologies, associated limitations, and key research gaps can highlight future research opportunities.

As such, the purpose of this scoping review was two-fold.

- 1) Synthesise evidence from large-scale urban studies that focused on the relation between urban structures, transport, environmental exposures, and health.
- 2) Advanced understanding of current knowledge and gaps, methodologies applied, limitations, and opportunities for the improvement of current research practice.

The research questions we sought to address were.

- 1) What methodologies were applied in urban form, transport and mobility, and urban environmental health studies from 2003 to 2023?
- 2) What are novel methods and indicators within urban environmental health research?

- 3) What knowledge gaps necessitate further exploration?

2. Methods

This review was conducted as part of The Urban Burden of Disease Estimation for Policy Making project (UBDPolicy). UBDPolicy aims to improve the estimation of health impacts and socio-economic costs, or benefits, of environmental determinants in almost 1000 European cities in 31 countries (Urban Burden of Disease Policy). Through provision of estimates of health impacts from air pollution (Khomenko et al., 2021), noise (Khomenko et al., 2022), heat (Jungman et al., 2023), and green space (Barboza et al., 2021) in regular three-yearly reporting intervals, UBDPolicy aims to advance understanding of wider impacts and trends from urban planning across Europe and build healthy and sustainable urban scenarios for specific case studies. Therefore, the conclusions drawn from this review and their applicability for UBDPolicy shaped the reasoning behind the methods employed. Given the exploratory nature required to meet the review's objectives, we conducted a scoping review suited to identifying knowledge gaps and emerging methods within a broad topic area (Peters et al., 2021). The anticipated heterogeneity of study designs of reviewed articles and practical and resource constraints rendered a systematic review or meta-analysis less suitable. Further, a UBDPolicy workshop held in Sitges, Spain, in October 2023 allowed expert consultation for identification of additional applicable studies. A literature search was performed using the bibliographical database PubMed. Fig. 2 provides a visual representation of the process of article inclusion and exclusion.

2.1. Keywords search process

Seven independent searches using PubMed were carried out (Table 1). The same search terms to describe urban form were included in the seven searches. The first search focused on urban form and health, the second on urban environmental health, and the third on urban indicators. The distinction between urban form and urban environmental health pertains to the former investigating the direct link between urban form and health whereas for the latter, studies consider the exposure pathway either by assessment of urban form to environmental exposures or exposures to health.

For the second category of urban environmental health studies, five searches encompassed the following key themes: air pollution and health impacts; temperature and health impacts; green space and health impacts; noise and health impacts; and transport and mobility. The searches returned 2958 unique articles (Fig. 2). Article abstracts were screened for relevance based on the inclusion criteria and objectives of UBDPolicy, which resulted in 40 papers for inclusion. An additional 26 papers were obtained from a manual search conducted by scanning reference lists for relevant studies and from expert consultation. This resulted in nine urban form and health studies 45 urban environmental health studies, and 12 urban indicator papers. A total of 66 studies were included. Table 1 provides a summary of the search terms used and results of each search. Fig. 3 categorises articles by theme and year of publication.

2.2. Inclusion criteria

Article inclusion criteria and conducted searches were divided into three search categories; urban form and health, urban environmental health (subdivided into HIA studies and other research methodologies), and urban indicators. For the second search category, a distinction of HIA methodologies was made to allow for effective exploration of methodologies and affiliated challenges within the broader urban environmental health field. The inclusion criteria for search categories one and two (urban form and health and urban environmental health studies) constituted studies were required to have analysed at least 90 cities, be written in English, and published in peer-reviewed journals

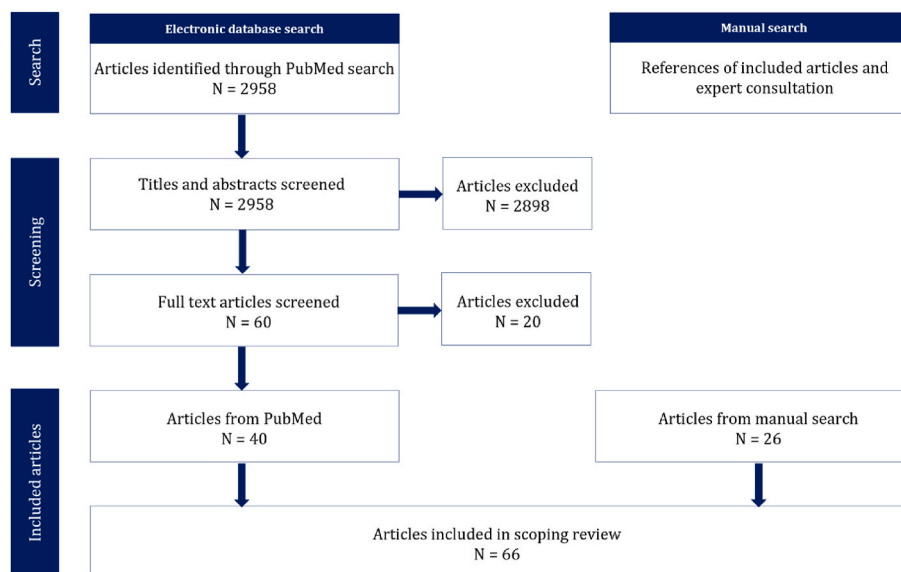


Fig. 2. Flowchart of the literature search inclusion and exclusion process.

from January 2003 to December 2023. The inclusion criterion was set at 90 or more cities as this number was considered appropriate to standardise data collection across different environmental and climatic gradients and to be representative of studies with less than 90 cities. Studies published from January 2003 to December 2023 were included to ensure methodologies and findings were reflective of current levels of urbanisation and health impacts. For the second search category of urban environmental health studies, the environmental exposures included were: air pollution; temperature; green space; road traffic noise; and transport and mobility.

The third search category focused on urban indicators. Indicators and frameworks considered relevant were those that focused on urban design and environmental health. The inclusion criteria specified studies should be written in English and published in peer-reviewed journals from January 2003 to December 2023.

2.3. Exclusion criteria

The exclusion criteria applied to both searches encompassed environmental exposures not relevant to UBDPolicy (such as infectious diseases), studies that did not evaluate health impacts, health outcomes considered less attributable to city design and planning, and studies published before January 2003. For the third search category of urban indicators, the exclusion criterion of studies analysing less than 90 cities did not apply, as indicators can be scaled and applied to different contexts.

3. Results

Of the 66 studies included in this review, the geographical regions covered were: Global (24), China (14), Europe (13), Latin America (9), the United States (3), and Africa (3) (Fig. 4 and Table 2). While studies specific to South-Asia, South-East Asia, and the Middle East were not considered in this review, a number of cities from these regions featured in the global studies. A total of 45 studies examined urban environmental exposures and health, with the majority (29, ~64%) assessing air pollution health impacts. The least studied exposure was road traffic noise (1, ~1.5%). The number of cities analysed spanned a wide range (93 - 13,189 cities), with variation in city definitions employed (Tables 3 and 4). All studies conducted in China examined the health effects from air pollution exposure, whereas less studied regions, such as Africa were amongst the largest in scale in terms of the number of cities analysed

(Fig. 4). Examination of findings is in accordance with the thematic order outlined in Table 2, and constitutes four sections: urban form and health, urban environmental health, HIAs, and urban indicators.

3.1. Urban form and health

Many studies that assessed urban form employed urban form metrics at city-level, namely: population density (Ortigoza et al., 2021; Bilal et al., 2021; Prieto-Curiel et al., 2017, 2023), fragmentation (Avila-Palencia et al., 2022a; Bilal et al., 2021), sprawl (Behnisch et al., 2022), built-up area (Avila-Palencia et al., 2022a; Behnisch et al., 2022), compact development (Taubenböck et al., 2020), intersection density (Avila-Palencia et al., 2022a), and mass transit infrastructure (Ortigoza et al., 2021; Avila-Palencia et al., 2022a). Fewer studies explored spatial observations and patterns within-city level (Prieto-Curiel et al., 2023; Taubenböck et al., 2020; Nguyen et al., 2019).

Health outcomes included long-term and short-term outcomes; long-term outcomes encompassed non-communicable diseases, cancer-related mortality, infant mortality, and mental distress, whilst short-term outcomes were violence-related and unintentional injury-related mortality (Table 3). The only urban form studies to include social and demographic variables in analyses were conducted in Latin America and employed the social environment index, which comprises area-level measures of education attainment, access to water and sewage facilities, and overcrowding (Bilal et al., 2021; Avila-Palencia et al., 2022a). Higher values indicate more favourable social conditions and a higher quality of life.

Findings suggest that lower city fragmentation, high population density, high connectivity, and higher rates of public transportation have positive impacts on health and reducing premature mortality (Ortigoza et al., 2021; Avila-Palencia et al., 2022a; Nguyen et al., 2019; Mullachery et al., 2022). Car-centric urban planning (Nguyen et al., 2019) was reported to have adverse effects on health, whilst in Africa greater sprawling cities were shown to have higher energy demands (Prieto-Curiel et al., 2023). City size was identified as the most critical variable for influencing urban sprawl with round and compact city designs generally more advantageous (Prieto-Curiel et al., 2023). Another African-based study conducted spatial analysis of four urban form variables in an effort to classify cities based on urbanisation dynamics (Prieto-Curiel et al., 2017). Prieto-Curiel et al. developed a systematic approach to capture and delineate the spatial interactions between variables of city size, market potential, level of urbanisation, and local

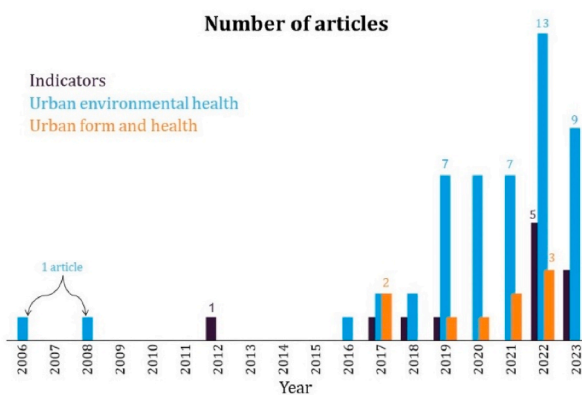


Fig. 3. Number of articles by published year and theme.

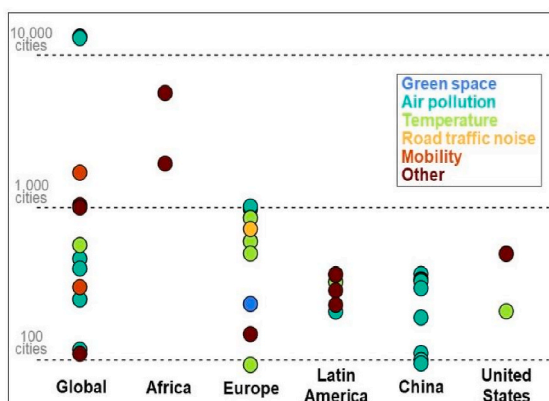


Fig. 4. Number of cities analysed in each study, categorised by region and environmental exposure.

Table 2
Summary of 66 included studies, by theme, geographic scope, and number of cities analysed.

Theme	Theme subcategory	Environmental Exposures	Number of studies	Geographical regions covered (Number of studies)	No. of cities Mean/Median (range)
Urban form and health	–	–	9	Global (2) Africa (2) Latin America (4) United States (1)	1046/363 (110–5625)
Urban environmental health	Urban environmental health	Air pollution	8	Global (4) China (1) Latin America (3)	312/346 (117–462)
		Temperature	6	Global (1) Europe (2) Latin America (2) United States (1)	447/500 (209–601)
		Green space	4	Africa (1) Europe (2) United States (1)	2118/496 (233–5625)
	Health Impact Assessment	Noise	–	–	–
		Transport and mobility	2	Global (2)	997 (301–1692)
		Air pollution	21	Global (6) China (13) Europe (2)	2048/335 (95–13189)
		Temperature	2	Europe (2)	474/474 (93–854)
		Green space	1	Europe (1)	978
		Noise	1	Europe (1)	724
Indicators	–	–	12	Global (9) Europe (3)	288/27 (14–1038)

increasing by 51% since 1990 (Behnisch et al., 2022).

3.2. Urban environmental health

Urban studies that investigated the exposure pathway to health in general followed an ecological (10, ~15%) or cross-sectional study design (6, ~9%), with a minority encompassing modelling studies (2, ~3%), or meta-analysis (1, ~1.5%) (Table 3). Certain studies adjusted for population demographic characteristics in their analyses, such as household income (Browning and Rigolon, 2018), income inequality (Bakhtsiyarava et al., 2023), self-rated health (Nguyen et al., 2019), educational attainment (Ortigoza et al., 2021), and race and ethnicity (Browning and Rigolon, 2018). Seven studies (~11%) directly examined the modification effect of socioeconomic status (SES) on the association between the urban environment and health, applying gross-domestic product (GDP) per capita (Gouveia et al., 2021; Kephart et al., 2023; Krummenauer et al., 2019), GINI coefficient (Bakhtsiyarava et al., 2023; Krummenauer et al., 2019), or GNI per capita (Rezaei and Millard-Ball, 2023). In all studies that performed stratified analyses of socioeconomic (SE) and demographics variables, aggregate data were applied at city-level.

3.2.1. Urban form and air pollution

Studies consistently reported significant proportions of urban populations to be exposed to ambient pollution that exceeded WHO 2005 (Anderson et al., 2022; Gouveia et al., 2021; Meng et al., 2021; Ye et al., 2021) and 2021 (Kephart et al., 2023; Heydari et al., 2022) guidelines. Findings from Latin America showed 85% of the study population exposed to ambient nitrogen dioxide (NO₂) concentrations and 58% exposed to PM_{2.5} levels that exceeded WHO guidelines (Gouveia et al., 2021; Kephart et al., 2023). Whilst Anderson et al. reported all the 5625 African cities under study failed to meet WHO 2005 clean air guidelines (Anderson et al., 2022).

The relation between city size, higher population density, and pollutant concentrations was somewhat inconsistent. A Latin American study reported larger population size was associated with higher annual mean PM_{2.5}, whilst higher population density was positively associated with lower levels of PM_{2.5} in a separate univariate model (Gouveia et al.,

Table 3
Summary of urban form, environment, and health studies that analysed at least 90 cities (cities analysed ranged from 110 to 5625).

Theme	Reference	Location (number of cities)	Study design	City definition	City database	Health outcome	Health data source	Environmental Exposure	Exposure data source	Urban form metric	Data source	Statistical method ^a
Urban form and health	Prieto-Curiel et al., 2017	Africa (1939)	Modelling	Continuously built-up area with <200m between two buildings and ≥10,000 inhabitants	Africapolis (OECD/SWAC. Africapolis database Internet, 2018)	–	–	–	–	City size Market potential Urbanisation level Local dominance	Africapolis (Moriconi-Ebrardi et al., 2016)	–
	Prieto-Curiel et al., 2017 (Prieto-Curiel et al., 2023)	Africa (5625)	Modelling	Continuously built-up area with <200m between two buildings and ≥10,000 inhabitants	Africapolis (OECD/SWAC. Africapolis database, 2018)	–	–	–	–	Building height Street network metrics Terrain metrics	Google AI Africa Open Buildings dataset	BASE model ^b
	Bilal et al., 2021	Latin America (363)	Ecological	Agglomerations of administrative units with ≥100,000 residents	SALURBAL study (Quistberg et al., 2019)	Cancer-related mortality CVD and other NCD-related mortality Unintentional injury-related mortality Violence-related mortality	Vital registration systems	–	–	City size City growth Population density Fragmentation Street connectivity Social environment index	SALURBAL study (Quistberg et al., 2019)	Nonparametric approach Three-level negative binomial multilevel model
Mullachery et al., 2022	Latin America (363)	Cross-sectional	Agglomerations of administrative units with ≥100,000 residents	SALURBAL study (Quistberg et al., 2019)	Healthcare-amenable mortality	–	SALURBAL study (Quistberg et al., 2019)	–	–	City population Fragmentation Patch density Population growth	SALURBAL study (Quistberg et al., 2019)	Log regression model

Main findings

- Spatial clustering classified seven city groups that showed distinct urbanisation dynamics and regional interactions.
- Spatial variables influenced urban growth rates, the emergence of urban agglomerations, and the clustering of cities.

Main findings

- Through estimation of interbuilding distances and urban form metrics, the cumulative effects of increased number of buildings, increased building size and sprawl were assessed.

- Estimated how increased urban commute times translates to required energy demand.

- When a city population doubles, energy demand from transport was found to triple.

Main findings

- Life expectancy and unintentional and violent injuries and deaths varied across cities, with large within-country variation.
- Causes of death from communicable, maternal, neonatal and nutritional, cancer, CVD and other NCDs varied substantially between countries.

- Rate ratios for each cause of death were associated with 1 standard deviation increase in city-level factors.

- Dense cities were found to have more violent deaths (relative to CVD and NCDs).

- Less fragmented and more connected cities had more communicable, maternal and neonatal and nutritional causes of deaths (relative to CVD and NCDs).

Main findings

- Urban population size and fragmentation were associated with amenable mortality.
- Regardless of fragmentation, population size was associated with higher amenable mortality.

- In small cities, higher urban fragmentation was associated with lower amenable mortality. In large cities, higher urban fragmentation was associated with higher amenable mortality.

- Population growth and higher SES (city-level) was associated with lower amenable mortality.

(continued on next page)

Table 3 (continued)

Theme	Reference	Location (number of cities)	Study design	City definition	City database	Health outcome	Health data source	Environmental Exposure	Exposure data source	Urban form metric	Data source	Statistical method ^a
	Nguyen et al., 2019	United States (500)	Cross-sectional	Categorised into tertiles	8	Obesity Diabetes Self-rated health Mental distress Physical distress Physical inactivity Teen births	BRFSS Survey Data (Centers for Disease Control and Prevention, 2014)	–	–	Highway Rurality Grassland	Google Street View	Linear regression models
	Ortigoza et al., 2021	Latin America (286)	Cross-sectional	Agglomerations of administrative units with ≥100,000 residents	SALURBAL study (Quistberg et al., 2019)	Infant mortality rate	Vital registration systems	–	–	Population size Population growth rate Living conditions score Services provision score Mass transit availability	SALURBAL study (Quistberg et al., 2019)	Poisson multilevel model
	Taubenböck et al., 2020 (Zhu et al., 2022)	Global (110)	Modelling	Morphological urban areas	United Nations (United Nations Department of Economic and Social Affairs Population Department, 2014)	–	–	Local Climate Zones	ESA (Agency TES, 2012)	–	–	–
	Avila-Palencia et al., 2022a	Latin America (230)	Cross-sectional	Agglomerations of administrative units with ≥100,000 residents	SALURBAL study (Quistberg et al., 2019)	NCD-specific mortality Unintentional injury-specific mortality	Vital registration systems	NDVI PM _{2.5} NO ₂ Carbon footprint	SALURBAL study (Quistberg et al., 2019)	Fragmentation Urban isolation Shape of patches	SALURBAL study (Quistberg et al., 2019)	Linear regression models
Air pollution and impacts	Meng et al., 2021	Global (398)	Ecological	–	(London School of Hygiene & Tropical Medicine)	All-cause mortality CVD mortality	Local authorities	NO ₂	(London School of Hygiene & Tropical Medicine)	–	–	Time series quasi-Poisson generalised linear regression

(continued on next page)

Table 3 (continued)

Theme	Reference	Location (number of cities)	Study design	City definition	City database	Health outcome	Health data source	Environmental Exposure	Exposure data source	Urban form metric	Data source	Statistical method ^a
						Main findings On average, 10 µg/m ³ increase in NO ₂ concentration on lag 1 previous day was associated with all-cause mortality (0.46%: 0.21–0.57%), CVD-related mortality (0.37%: 0.22–0.51%) and respiratory-related mortality (0.47%: 0.21–0.72%). - Associations remained robust after adjusting for co-pollutants (PM ₁₀ < 10 µg/m ³ and PM _{2.5} < 2.5 µg/m ³ , ozone, SO ₂ and CO).						model meta-analytical approach Random Forests model
	Ye et al., 2021)	China (367)	Ecological	Boundaries defined in the Population Census	China Health Statistical Yearbook (Chinese Statistical Yearbook, 2020)	All-cause mortality	China Health Statistical Yearbook (Moriconi-Ebrardi et al., 2016)	PM _{2.5} PM ₁₀ CO ₂ NO ₂ SO ₂ TSP	China's National Urban Air Quality Real-time Publishing Platform (China National Urban Air Quality Real-time Publishing Platform, 2020)	–	–	
						Main findings - Compared air quality during the COVID lockdown period in early 2020 with a business-as-usual scenario and found: 1239 (844–1578) PM _{2.5} related avoidable deaths; economic savings 1.22 billion USD. 2777 (1565–3995) PM ₁₀ related avoidable deaths; economic savings 2.60 billion USD. 1587 (98–3104) CO related avoidable deaths; economic savings 1.36 billion USD. 4711 (3649–5781) NO ₂ related avoidable deaths; economic savings 4.05 billion USD. 213 (116–314) O ₃ related avoidable deaths; economic savings 0.20 billion USD. 1088 (774–1421) SO ₂ related avoidable deaths; economic savings 0.95 billion USD.						
	Kephart et al., 2023	Latin America (326)	Cross-sectional	Clusters of administrative units encompassing an urban built-up area ^a	SALURBAL study (Quistberg et al., 2019)	–	–	NO ₂ NDVI	SALURBAL study (Quistberg et al., 2019) US Geological Survey (MODIS MOD13Q1) (Didan, 2015)	Population density Intersection density GDP per capita Traffic congestion	SALURBAL study (Quistberg et al., 2019) Kummu et al., 2017 (Kummu et al., 2018) Delclòs-Alió et al., 2019 (Delclòs-Alió et al., 2022)	Multilevel models
						Main findings – 85% of the study population (almost 9 out of 10 residents) were exposed to ambient NO ₂ concentrations that exceeded current WHO guidelines. - Larger, denser, and more congested cities had higher NO ₂ concentrations. - Higher population density was independently associated with higher NO ₂ concentrations (city and neighbourhood levels). - Greenness was associated with lower NO ₂ at neighbourhood level (not city-level). - Found a positive association between educational attainment (neighbourhood level) and ambient NO ₂ concentrations.						
	Heydari et al., 2022	Global (117)	Meta-analysis	–	–	COPD Diabetes IHD Lower respiratory disease Lung cancer Stroke	GBD 2017 (Stanaway et al., 2017)	PM _{2.5}	WHO (World Health Organisation, 2015)	–	–	Non-linear Integrated Exposure Response function
						Main findings - Eliminating traffic emissions was estimated to achieve WHO 2021 recommended PM _{2.5} levels for 25 cities, that had low current PM _{2.5} concentrations. - For cities with up to 30–40 µg/m ³ of PM _{2.5} concentrations, the benefits of preventable mortality showed an increasing trend. After this threshold large variations in preventable mortality were observed. - The percentage reduction in diabetes-related mortality decreased with increasing PM _{2.5} concentrations (an opposing trend to other outcomes under study). - The IER functions of PM _{2.5} showed reduced health benefits at higher concentrations. - The shape of IER functions had a significant effect on health benefits.						

(continued on next page)

Table 3 (continued)

Theme	Reference	Location (number of cities)	Study design	City definition	City database	Health outcome	Health data source	Environmental Exposure	Exposure data source	Urban form metric	Data source	Statistical method ^a
Temperature and impacts	Kephart et al., 2022 (Centers for Disease Control and Prevention c.)	Latin America (326)	Ecological	Agglomerations of administrative units with $\geq 100,000$ residents	SALURBAL project (Quistberg et al., 2019)	All-cause mortality CVD-related mortality Respiratory disease-related mortality Respiratory infection-related mortality	Vital registration systems	Ambient air temperature	ERA5-Land (Muñoz-Sabater et al., 2021)	–	–	Distributed lag nonlinear conditional Poisson model Random effects meta-regression model
	Wang et al., 2016	United States (209)	Ecological	–	–	Mortality	National Centre for Health Statistics	Cold waves ^c	CMIP Phase 5 ¹⁰¹	–	–	Over-dispersed Poisson regression
	Krummenauer et al., 2019	Europe (599)	Ecological	≥ 1500 inhabitants per km (The World Bank)	Gridded population of the world (Centre for International Earth Science Information Network (CIESIN), 2016)	Life expectancy Health expenditure	WBOD (The World Bank, 2016) World Income Inequality Database) MDGLR (United Nations Development Programme, 2008)	Minimum mortality temperature	Global Summary of the Day (NOAA National Climatic Data Center, 2018)	Topography Population density GDP per capita GINI coefficient Improved water source	CIESIN (Centre for International Earth Science Information Network (CIESIN), 2016)	Non-linear sigmoid model
	Alahmad et al., 2023	Global (567)	Ecological	–	MCC (London School of Hygiene & Tropical Medicine)	CVD-specific mortality data	(London School of Hygiene & Tropical Medicine)	Ambient temperature	MCC (London School of Hygiene & Tropical Medicine)	–	–	Case-crossover models Mixed-effects meta-analytic framework

Main findings

- Overall, higher proportion of deaths were attributable to ambient cold compared to ambient heat.
- Risks were strongest among older adults and for CV- and respiratory-related deaths.
- RR 1.057 (1.046–1.067) per 1 °C higher temperature during extreme heat.
- RR 1.034 (1.028–1.040) per 1 °C lower temperature during extreme cold.
- For heat-related deaths, 0.67% (0.58–0.74) excess death fraction of total deaths.
- For cold-related deaths, 5.09% (4.64–5.47) excess death fraction of total deaths.

Main findings

- Cold waves were associated with a small increase in risk of mortality.
- Lingering effects of cold waves were larger than the cold waves themselves.
- Risk increased with duration and intensity of cold waves, however decreased with mean winter temperature.
- Associations varied substantially across climatic regions.

Main findings

- MMT was found to be influenced by topography and SE factors.
- There was lower MMTs in cities with higher altitudes.
- There was a positive association between higher SE indicators with MMT, suggesting higher SES increases an urban population's adaptive capacity to heat.
- Other climatic, topographic, demographic and SE factors were not significant predictors of MMT.

Main findings

- Extreme heat and cold were associated with a higher risk of dying from any CVD-cause, IHD, stroke, and HF compared to MMT.
- Excess CVD deaths from sustained extreme cold were larger than those from extreme heat.
- For every 1000 HF deaths, hot days accounted for 2.6 (2.4–2.8) deaths and cold days accounted for 12.8 (12.2–13.1) deaths.
- For every 1000 CVD deaths, cold days (below 2.5th percentile) accounted for 9.1 (8.9–9.2) and hot days (above 97.5th percentile) accounted for 2.2 (2.1–2.3).

(continued on next page)

Table 3 (continued)

Theme	Reference	Location (number of cities)	Study design	City definition	City database	Health outcome	Health data source	Environmental Exposure	Exposure data source	Urban form metric	Data source	Statistical method ^a
	Bakhtsiyarava et al., 2023	Latin America (325)	Ecological	Agglomerations of administrative units with ≥100,000 residents	SALURBAL study (Quistberg et al., 2019)	All-cause mortality CVD-specific mortality	Vital registration systems SALURBAL study (Quistberg et al., 2019)	Temperature	ERA5-Land (Muñoz-Sabater et al., 2021)	–	–	Distributed lag nonlinear conditional Poisson model Random effects meta-regression model
	Zhou et al., 2017	Europe (5000)	Ecological	Urban agglomerations	CORINE land cover (Copernicus, 2012a,b)	–	–	Surface UHI intensity	CMIP Phase 5 ¹⁰¹	City size Urban fractality Urban anisometry	CORINE morphological zones (European Environment Agency, 2006)	Multi-linear regression model
	Marando et al., 2022	Europe (601)	Modelling	Functional Urban Areas	GHSL (European Commission's Joint Research Centre)	–	–	Land surface temperature	Google Earth Engine (Parastatidis et al., 2017)	Cooling index ^d	Copernicus (Copernicus, 2018a) MODIS (Didan, 2015)	Bivariate linear regression model Univariate model
Green space	Browning and Rigolon, 2018	United States (496)	Cross-sectional	–	500 Cities project (Centers for Disease Control and Prevention a.)	Obesity Mental health	500 Cities project (Centers for Disease Control and Prevention a.)	NDVI Tree cover	MODIS (Wickham et al., 2014) Multi-Resolution Land Characteristics Consortium (Consortium, 2011)	–	–	Spatial moving average models
	Anderson et al., 2022 (World Climate	Africa (5625)	Modelling	Continuously built-up area with <200m between two buildings and	Africapolis (OECD/SWAC. Africapolis database. 2018)	–	–	Urban green space fraction Proximity to	WorldClim, 2020) GHSL (Schiavina M. and KM, 2019)	Urban form metrics ^e	European Space Agency's World Cover Map (Zanaga et al., 2021)	Linear econometric models

Main findings

- Greater excess mortality was associated with cold temperatures (below MMT): 5.09% (4.64–5.47) compared to excess mortality associated with heat (temperatures above MMT): 0.67% (0.58–0.74%).
- There was limited effect modification of demographic and SE characteristics (city-level) of cold-related mortality.
- GINI index of income inequality was the only modifier to show a statistically significant association with all-age, cold-related mortality (3.45 [CI 0.33, 6.56] percentage-points higher compared to cities with a low GINI index).
- Higher levels of poverty was associated with lower heat-related mortality: cities in the top tertile of population density had heat EDF 0.70 [CI 1.16, –0.25] percentage-points lower than cities in the bottom tertile.
- Higher income inequality was associated with lower heat-related mortality: cities in the top tertile of the GINI index had heat EDF 1.16 [CI 1.90, –0.43] percentage-points lower than cities with the smallest GINI index.

Main findings

- Larger and more compact cities (high urban fractality) with less sprawl (small anisometry) had the strongest UHI intensities.
- City size had the strongest influence on UHI, followed by fractality.
- There was a complex interplay between urban form factors and UHI.

Main findings

- Tree cover of at least 16% was required to achieve a reduction of 1 °C in urban temperatures.
- 32% of European FUAs had tree cover below 16%.
- The impact of trees on reducing UHI is dependent on the extent of green areas and amount of transpiration inside a city.
- In almost 40% of the countries under study, more than half of the resident population do not benefit from the microclimate regulation provided by urban tree coverage.

Main findings

- Greener cities had less obesity and better mental health outcomes.
- No evidence that tree cover was more strongly linked to positive health outcomes compared to greenness.
- Cities with lower median household income had greater benefits from green space compared to wealthier cities.
- Sprawl did not have a moderating effect on the greenspace-health link.
- Regardless of a city's population density, tree cover was linked to better obesity outcomes and overall greenness was linked to better mental health outcomes.

(continued on next page)

Table 3 (continued)

Theme	Reference	Location (number of cities)	Study design	City definition	City database	Health outcome	Health data source	Environmental Exposure	Exposure data source	Urban form metric	Data source	Statistical method ^a
	Research Programme)			≥10,000 inhabitants				green space PM _{2.5}				
	Olsen et al., 2019	Europe (233)	Cross-sectional	Large Urban Zones of ≥100,000 inhabitants	Urban Atlas 2018 (Copernicus. Urban Atlas, 2018c)	All-cause mortality (SMR)	Richardson et al., 2017	–	–	Land cover uses ^f	See supplementary (Olsen et al., 2019)	Linear regression models
Transport and mobility	Thompson et al., 2020	Global (1692)	Cross-sectional	1) Minimum radius of 1.5 km 2) Selected images of 400m ²	United Nations (Bassolas et al., 2019) Google Static Maps	Road traffic injuries (DALYs, YLLs, YLDs)	GBD 2016 (Centers for Disease Control and Prevention a)	Fossil fuel emissions	FFDAS (Wickham et al., 2014)			2 x 3 multivariate analysis of variance
	Bassolas et al., 2019	Global (301)	Ecological	Metropolitan areas	U.S. Census	Stroke (incidence) Stroke-related mortality Transport-related mortality	CDC (Centers for Disease Control and Prevention b.) (U.S. Department of Transportation)			Trip flow data	Mobility Map project (Kirmse et al., 2011)	Multivariate analysis

Abbreviations: Cardiovascular disease (CVD); Non-communicable disease (NCD); Social economic status (SES); Behavioural Risk Factor Surveillance System (BRFSS); Infant mortality rate (IMR); Normalised differential vegetation index (NDVI); Multi-City Multi-Country Collaborative Research Network (MCC); Terra Moderate Resolution Imaging Spectroradiometer (MODIS) Vegetation Indices (MOD13Q1); Chronic obstructive pulmonary disorder (COPD); Ischaemic heart disease (IHD); Global Human Settlement Layer (GHSL); Hypertension (HTN); Coupled Model Intercomparison Project Phase 5 (CMIP5); World Bank Open Data (WBOD); Millennium Development Goals Lebanon Report (MDGLR); Centre for International Earth Science Information Network (CIESIN); Urban Heat Island (UHI); Standardised mortality rate (SMR); Disability-adjusted life years (DALYs); Years of life lost (YLLs); Years lived with disability (YLDs); Fossil Fuel Data Assimilation System (FFDAS).

^a Statistical method for estimation of association between urban form, exposures, and health.

^b BASE model: mean distance between buildings is a functional relation to the number of Buildings and their average Area and the Sprawl and the Elongation of its spatial arrangement. Allows relation of city morphology to distance indicators (e.g., sprawl, elongation, and polycentricity) and the energy demand from transport.

^c Cold waves defined as two, three, or at least four consecutive days with daily temperature lower than the 5th percentile of temperatures recorded in each city.

^d Variables included in cooling index: tree cover density, water evaporation from tree canopies, vaporisation of intercepted rainfall from vegetation.

^e Urban form metrics include sprawl, city elongation, built-up intensity, intersection density, average node degree, city centre building density, types of green cover, total footprint centre 1 km, is pyramid, urban green space fraction.

^f Land covers/uses include agriculture, semi-natural areas, wetlands, green urban areas, industrial, commercial, public, military, discontinuous low density urban fabric, residential, isolated structures.

2021). Another Latin American study reported denser and more congested cities to have higher NO₂ and PM_{2.5} concentrations, owing to higher motorisation rates and congestion (Kephart et al., 2023). The same study reported highest variability in NO₂ population exposure was within cities and an increase in green space at neighbourhood level, rather than city-level, was associated with lower local levels of NO₂⁶⁰. Interestingly, Rezaei & Millard-Ball observed cities with greater density exhibited reduced per capita PM_{2.5} transportation emissions; however, increased exposure was noted due to the population residing in closer proximity to emission sources (Rezaei and Millard-Ball, 2023). Authors noted greater variation in emission exposure between income groups, as opposed to urban form metrics and income where no significant correlations were found. Another study found higher city GDP per capita and higher intersection density correlated with elevated levels of PM_{2.5}⁵⁹. The only study to include educational attainment in analyses found population groups of higher educational attainment were exposed to higher NO₂ concentrations (Kephart et al., 2023).

3.2.2. Urban form and temperature

Studies that assessed the relationship between urban form, temperature, and health mainly focused on the impact of non-optimal temperatures on premature and cardiovascular-related mortality (Bakhtsiyarava et al., 2023; Alahmad et al., 2023; Kephart et al., 2022). In Europe, lower minimum mortality temperature (MMT) positively correlated with lower GDP per capita; for example, spatially close cities of Austria (Vienna) and Slovakia (Bratislava) exhibited MMTs of 20.5 °C and 18.4 °C and GDP per capita of 29,301 and 11,348, respectively (Krummenauer et al., 2019). A Latin American study found the GINI coefficient, indicative of income inequality, was the sole modifier that showed a statistically significant association with all-age MMT (Bakhtsiyarava et al., 2023). Cities exhibiting the highest income inequality experienced a mortality rate 3.45% higher than those in the lowest tertile of income inequality (Bakhtsiyarava et al., 2023). For ages 65 years and older, increased levels of poverty and residential segregation were linked to higher cold MMT (Bakhtsiyarava et al., 2023). Of note, there were higher deaths associated with cold, 5.09% out of 5.75% non-optimal temperature attributable deaths at all ages, compared to 0.67% deaths associated with heat (Bakhtsiyarava et al., 2023). Zhou et al. found city size and compactness to have the strongest influence on UHI intensities, concluding small to medium sized cities were most effective in alleviating UHI (Zhou et al., 2017).

3.2.3. Urban form and green space

Generally, studies found the health benefits of urban green space to depend upon the distribution within a city (Browning and Rigolon, 2018; Rezaei and Millard-Ball, 2023; Avila-Palencia et al., 2022b). Reported health benefits included lower levels of obesity (Browning and Rigolon, 2018; Avila-Palencia et al., 2022b), mental health disorders (Browning and Rigolon, 2018), and lower pollutant levels (Anderson et al., 2022; Kephart et al., 2022). Across African cities, linear econometric models predicted the impact of increasing green space cover by at least 25% and found this would reduce PM_{2.5} to moderately safe levels (12–35.4 µg/m³) (Anderson et al., 2022). Evidence varied on whether the type of green space had an effect on benefits. Olsen et al. explored a range of land uses and the impacts at individual and aggregate city-level across European cities and found relatively wild green space (constituting agricultural, wetlands, and semi-natural areas) was associated with lower standardised mortality rate (Olsen et al., 2019). Another study found a significant correlation between poor mental health and greenness and between obesity and tree cover, reporting no significant relationships between greenness and obesity, or between tree cover and mental health (Browning and Rigolon, 2018). A notable strength of Browning et al.'s study was the inclusion of moderation tests for exploring effect modification, analysing sociodemographic variables and urban sprawl (defined by population density, the percentage who drive to work, and residential density). When adjusting for spatial and

Table 4
Summary of health impact assessments that analysed at least 90 cities (cities analysed ranged from 93 to 13,189).

Reference	Location (number of cities)	City definition	City population database	Outcome	Outcome data source ^a	Temporal resolution	Environmental exposure (Resolution Scale) ^b	Environmental exposure data source	Relative Risk	ERF data Source ^c	Models to estimate exposure	Counterfactual Scenario
Khomenko et al., 2021	Europe (1016)	Local administrative boundaries, with ≥50,000 inhabitants (European Commission's Joint Research Centre)	Urban Audit (Eurostat)	Natural cause mortality (rate per 100,000 and YLL)	Eurostat (European Commission, 2019) (City-level)	2015	PM _{2.5} NO ₂ (100m ²)	ELAPSE (de Hoogh et al., 2018)	PM _{2.5} -1.07 (1.04–1.09) per 10 µg/m ³ increase NO ₂ -1.02 (0.99–1.06) per 10 µg/m ³ increase	(World Health Organization, 2014 ; Atkinson et al. (2018))	LUR model (100m ²) Ensemble model (10 km (The World Bank)) Global LUR model (100m ²)	PM _{2.5} -10 µg/m ³ NO ₂ - 40 µg/m ³
Khomenko et al., 2023	Europe (857)	Local administrative boundaries, with ≥50,000 inhabitants (European Commission's Joint Research Centre)	Urban Audit (Eurostat ^d)	Natural cause mortality	Eurostat (Guan et al., 2021b) (City-level)	2015	PM _{2.5} NO ₂ (0.1° × 0.05° / ~6 km (The World Bank))	Copernicus Atmosphere Monitoring Service regional inventory (Kuenen et al., 2022)	PM _{2.5} -1.08 (1.06–1.09) per 10 µg/m ³ increase NO ₂ -1.02 (1.01–1.04) per 10 µg/m ³ increase	(Chen and Hoek, 2020 ; Huangfu and Atkinson (2020))	SHERPA tool (European Commission) EMEP MSC-W chemical transport model (Simpson et al., 2012 ; Pisoni et al., 2019)	Pollutant concentrations related to each emission source eliminated
(Anenberg et al., 2019a)	Global (250)	Population census tables and corresponding geographic boundaries	(Centre for International Earth Science Information Network (CIESIN), 2016)	All-cause mortality IHD Stroke COPD Lung cancer Lower respiratory infections Diabetes	GHDx (Kuenen et al., 2022) (0.1° × 0.1° grid cell level)	2010 and 2015	PM _{2.5} Ozone (0.1° × 0.1° / ~10 km (The World Bank))	ECLIPSE (Klimont et al., 2017 ; Stohl et al., 2015)	See references (Shaddick et al., 2018 ; Stanaway et al., 2017)	(Shaddick et al., 2018) GBD 2017 (Stanaway et al., 2017)	GEOS-Chem global chemical transport model (2° × 2.5°)	PM _{2.5} -2.4–5.9 µg/m ³ Ozone- 32.4 ppb (~63.5 µg/m ³)
Zhang et al., 2022	China (331)	Defined by the Population Census	China Health Statistical Yearbook (China economic and social big, 2020)	Premature mortality CVD mortality Respiratory mortality	China Health Statistical Yearbook (China economic and social big, 2020)	2015–2020	PM _{2.5} Ozone	China National Environmental Monitoring Centre (Copernicus Urban Atlas, 2018c)	ERF reported (Zhang et al., 2022)	(Kan and Chen, 2002)	Univariate linear regression model	PM _{2.5} -10 µg/m ³ Ozone- 26.7 ppb (~54 µg/m ³)
(Guan et al., 2021b)	China (338)	Defined by the Population Census	National Bureau of Statistics of China (National Bureau of Statistics of China, 2021)	All-cause mortality (DALY) Respiratory disease (DALY)	GBD Study 2016 (Naghavi et al., 2017) (Provincial level)	2015–2020	PM _{2.5} Ozone	China National Environmental Monitoring Centre (Ministry of Environmental Protection)	All-cause ozone – 1.01 per 10 µg/m ³ increase Respiratory disease ozone – 1.02 per 10 µg/m ³ increase	Burnett et al., 2014 Maji et al., 2018 (Wang et al., 2021)	-	PM _{2.5} -10, 15, 25, 35 µg/m ³ Ozone – 100, 160 µg/m ³ (~196, 313.6 ppb)
(Guan et al., 2021a)	China (101)	City seasonal population	Baidu population migration index (Baidu Map)	CVD (DALYs) Respiratory disease (DALYs)	GBD Study 2017 (Zhou et al., 2019) (Provincial level)	Fourteen seasons from 2017, 2018, 2019 and first half of 2020	PM _{2.5} Ozone	(China National Environmental Monitoring Centre, 2020)	See Table 1 of Appendix (Guan et al., 2021a)	-	-	PM _{2.5} -25 µg/m ³ Ozone- 100 µg/m ³ (~196 ppb)
(Guan et al., 2022a)	China (335)	Defined by the Population Census	(National Bureau of Statistics of China, 2021)	All-cause (DALY) CVD (DALY) Respiratory disease (DALY)	GBD Study 2017 (Zhou et al., 2019) (Provincial level)	2021	PM _{2.5} Ozone	(China National Environmental Monitoring Centre, 2020)	-	Orellano et al., 2020	-	PM _{2.5} -15 µg/m ³ Ozone- 70 µg/m ³ (~137.2 ppb)

(continued on next page)

Table 4 (continued)

Reference	Location (number of cities)	City definition	City population database	Outcome	Outcome data source ^a	Temporal resolution	Environmental exposure (Resolution Scale) ^b	Environmental exposure data source	Relative Risk	ERF data Source ^c	Models to estimate exposure	Counterfactual Scenario
(Anenberg et al., 2019b)	Global (250)	≥1500 inhabitants per km (The World Bank)	CIESIN (Centre for International Earth Science Information Network (CIESIN), 2016)	Mortality	GBD 2016 (Stanaway et al., 2017)	2016	PM _{2.5} ((~0.0083°) (The World Bank) /1 km (The World Bank)) CO ₂ (1 km (The World Bank))	Shaddick et al., 2018 Oda and Maksyutov, 2011	Age-specific RR ^c	Cohen et al., 2017	Chemical transport model (Calibrated to 6003 measurements for 117 countries)	2.4–5.9 µg/m ³
Maji et al., 2017	China (190)	Defined by the Population Census	(National Bureau of Statistical of China, 2016; Zhang and Cao, 2015)	All-cause mortality 5 causes premature mortality 18 causes morbidity	GBD Study 2010 (Naghavi et al., 2017) (Provincial level)	2014–2015	PM _{2.5} PM ₁₀	GBD 2010 (Institute for Health Metrics and Evaluation GHDX, 2010)	See Table 1 ¹³³	GBD 2010 (Naghavi et al., 2017)	–	PM _{2.5} –20 µg/m ³ PM ₁₀ –5.8 µg/m ³
Maji et al., 2018	China (338)	Defined by the Population Census	(National Bureau of Statistical of China, 2016)	Stroke IHD COPD Lung cancer Cause-related hospital admission	GBD Study 2016 (Naghavi et al., 2017) (Provincial level)	2016	PM _{2.5}	(China National Environmental Monitoring Centre, 2020)	–	–	–	PM _{2.5} –5.9 µg/m ³
Guan et al., 2019	China (328)	Defined by the Population Census	(National Bureau of Statistical of China, 2016)	CVD mortality Respiratory disease mortality Lung cancer mortality	Zhou et al., 2016 (Provincial level)	2015–2017	PM _{2.5}	(China National Environmental Monitoring Centre, 2020)	–	–	–	PM _{2.5} –10 µg/m ³
Diao et al., 2020	China (338)	Defined by the Population Census (National Bureau of Statistical of China, 2016)	China Health Statistical Yearbook (China economic and social big, 2020)	All-cause mortality Respiratory mortality CVD hospitalisation Chronic bronchitis hospitalisation Asthma diagnosis Acute bronchitis diagnosis	–	2015	PM _{2.5}	LandScan (Dobson et al., 2000)	All-cause mortality PM _{2.5} ^c 1.019 (1.003–1.081) per 10 µg/m ³ increase See Table 1 for full list (Diao et al., 2020)	Wang et al., 2017	–	PM _{2.5} –10 µg/m ³
Han et al., 2022	China (296)	Population census tables and corresponding geographic boundaries	(Centre for International Earth Science Information Network (CIESIN), 2016)	All-cause mortality	China Health Statistical Yearbook (China economic and social big, 2020) (City-level)	2015–2019	PM _{2.5} (0.1° × 0.1° /~10 km (The World Bank))	Satellite sources (Geng et al., 2021) Emission-inventories (TAP [Internet]) Model simulation (Xiao et al., 2021a) Ground-based sources (Xiao et al., 2021b)	All-cause mortality PM _{2.5} ^c 1.055 (1.022–1.088) (Guan et al., 2021b) per 10 µg/m ³ increase	Zhang, 2021 (Centers for Disease Control and Prevention b.)	Artificial intelligence combined data from satellite-, emission inventories-, model simulation- and ground-based sources.	PM _{2.5} –5 µg/m ³

(continued on next page)

Table 4 (continued)

Reference	Location (number of cities)	City definition	City population database	Outcome	Outcome data source ^a	Temporal resolution	Environmental exposure (Resolution Scale) ^b	Environmental exposure data source	Relative Risk	ERF data Source ^c	Models to estimate exposure	Counterfactual Scenario
Southerland et al., 2022	Global (13,160)	Defined by Global Human Settlement Model grid (Dijkstra et al., 2021)	European Commission's Joint Research Centre (Pesaresi et al., 2019)	Attributable cause-specific mortality of: Ischaemic heart disease Intracerebral haemorrhagic stroke Lower-respiratory infections Lung cancer Type 2 diabetes COPD	GBD 2019 (Abbfati et al., 2020) (National level)	2000–2019	PM _{2.5} ((~0.0083°) ² /1 km ²)	PM _{2.5} concentration database (Hammer et al., 2020)	Produced RR estimates for 385 integer exposure levels ranging from 0 to 2500 µg/m ³	Zheng et al., 2021 (Centers for Disease Control and Prevention b.)	Integrated data from satellite-retrieved aerosol optical depth, chemical transport modelling, and ground monitor data.	PM _{2.5} -2.4–5.9 µg/m ³
Zhang et al., 2008	China (111)	Defined by the Population Census	China Health Statistical Yearbook	All-cause mortality CVD hospitalisation Chronic bronchitis Acute bronchitis Respiratory hospitalisation Asthma attack Outpatient visits (internal medicine) Outpatient visits (paediatric)	China Health Statistical Yearbook (China economic and social big, 2020) (Provincial level)	2004	PM ₁₀	SEPAC (State Environmental Protection Administration of China (SEPAC), 2005)	ERF reported (Zhang et al., 2008)	–	–	PM ₁₀ - 40 µg/m ³
(Malashock et al., 2022a)	Global (12,946)	Population of ≥0.05 million and ≥1500 inhabitants per km (The World Bank), or built up area of at least 50% and town population between 20000-50000 ¹⁸³	European Commission's Joint Research Centre (Pesaresi et al., 2019)	Attributable cause-specific mortality	GBD 2019 (Abbfati et al., 2020) (National level)	2000–2019	Ozone ((~0.0083°) ² /1 km ²)	OSDMA8 (Delang et al., 2021)	Respiratory mortality-1.06 per 10 ppb ozone	Turner et al., 2016	–	Ozone- 32.4 ppb ¹⁸⁸ (~63.5 µg/m ³)
(Guan et al., 2022b)	China (338)	Defined by the Population Census	China Health Statistical Yearbook	All-cause mortality Respiratory mortality COPD mortality	GBD Study 2017 (Zhou et al., 2019) (Provincial level)	2015–2020	Ozone NO ₂ (0.25° × 0.25°)	(China National Environmental Monitoring Centre, 2020)	–	Anenberg et al., 2018 Huangfu and Atkinson, 2020	–	WHO 2021 guidelines (WHO. WHO global air quality guidelines: Particulate matter, 2021)
Maji et al., 2019	China (338)	Defined by the Population Census	China Health Statistical Yearbook (China's	CVD mortality Respiratory mortality	GBD Study 2016 (Naghavi et al., 2017) (Provincial level)	2016	Ozone	(China National Environmental Monitoring Centre, 2020)	Respiratory mortality-1.04 (1.013–1.067) per 20 mg/m ³ increase	Jerrett et al., 2009	–	Ozone- 75.2 µg/m ³ (~38.34 ppb)

(continued on next page)

Table 4 (continued)

Reference	Location (number of cities)	City definition	City population database	Outcome	Outcome data source ^a	Temporal resolution	Environmental exposure (Resolution Scale) ^b	Environmental exposure data source	Relative Risk	ERF data Source ^c	Models to estimate exposure	Counterfactual Scenario
			economic and social big, 2020)						CV mortality-1.01 (1–1.2) per 20 mg/m ³ increase			
Mead and Brajer, 2006)	China (95)	Defined by the Population Census	China Environmental Yearbook	Non-accident mortality	Author derived (City-level)	2001	NO ₂ SO ₂ TSP	China Environmental Yearbook	NO ₂ (The World Bank)- 1.012 and 1.008 SO ₂ - 1.0188 TSP- 1.013	–	–	NO ₂ -80 and 40 µg/m ³ SO ₂ - 60 and 50 µg/m ³ TSP- 200 and 90 µg/m ³
Anenberg et al., 2022	Global (13,189)	Defined by Global Human Settlement Model grid	European Commission's Joint Research Centre (Pesaresi et al., 2019)	Paediatric asthma incidence	GBD 2019 study (Abbafati et al., 2020) (National level)	1990–2019	NO ₂ ((~0.0083°) ² /1 km ²)	Adjusted existing model (Larkin et al., 2017)	1.26 (1.1–1.37) per 10 ppb annual average increase	Achakulwisut et al., 2019	LUR model (100m ²)	NO ₂ - < 2 ppb (~3.78 µg/m ³)
Song et al., 2023	Global (13,189)	Defined by Global Human Settlement Model grid	European Commission's Joint Research Centre (Pesaresi et al., 2019)	All-cause mortality	GBD 2019 study (Abbafati et al., 2020) (City-level)	2019	NO ₂ (1 km (The World Bank))	Dataset from Anenberg et al., 2022	1.047 (1.023–1.072) per 10 ppb increase	Stieb et al., 2021)	LUR model (Anenberg et al., 2022)	10 µg/m ³ (~5.32 ppb)
Barboza et al., 2021	Europe (978)	Local administrative boundaries, with ≥50,000 inhabitants (China National Urban Air Quality Real-time Publishing Platform, 2020)	Urban Audit (Institute for Health Metrics and Evaluation)	Natural-cause mortality (rate per 100,000 and YLL)	Eurostat (Maji et al., 2019) (City-level)	2015	NDVI %GA (250m ²)	US Geological Survey (MODIS MOD13Q1) (United States Census Bureau, 2016) European Urban Atlas (Southerland et al., 2022)	%GA–0.99 (0.98–1.01) for every 10% increase in GA NDVI–0.96 (0.94–0.97) for every 0.1 unit increase in green exposure	Gascon et al., 2016 (Jerrett et al., 2009) Rojas-Rueda et al., 2019 (Larkin et al., 2017)	–	%GA– 25% GA within 300m of residence Target NDVI estimated per city (Cerin et al., 2013)
lungman et al., 2023	Europe (93)	Local administrative boundaries, with ≥50,000 inhabitants (European Commission's Joint Research Centre)	Urban Audit (Eurostat ^a)	All-cause mortality (rate per 100,000 and YLL)	(Eurostat, 2015) (City-level)	2015	Heat (UHI) (100m ²) Tree cover density (250m ²)	Copernicus Urban Climate dataset (Copernicus, 2018b) Copernicus tree coverage (Copernicus Land Monitoring Service)	City and age-specific ERFs; supplementary (lungman et al., 2023)	Masselot et al., 2023	–	Day-time UHI- 0.6 °C Night-time UHI- 1.9 °C Tree coverage: 25%, 30%, 40%
Masselot et al., 2023	Europe (854)	Local administrative boundaries, with ≥50,000 inhabitants (European Commission's Joint Research Centre)	Urban Audit (Eurostat ^a)	All-cause mortality Non-accidental causes of mortality	Eurostat (European Commission, 2019) MCC Collaborative Research Network (London School of Hygiene & Tropical Medicine) (City-level)	2000–2020 ^d	Extreme heat Extreme cold (9 km (The World Bank))	ERA5-Land dataset (Muñoz-Sabater et al., 2021)	City and age-specific ERFs; see supplementary (Masselot et al., 2023)	Masselot et al., 2023	–	–

(continued on next page)

Table 4 (continued)

Reference	Location (number of cities)	City definition	City population database	Outcome	Outcome data source ^a	Temporal resolution	Environmental exposure (Resolution Scale) ^b	Environmental exposure data source	Relative Risk	ERF data Source ^c	Models to estimate exposure	Counterfactual Scenario
Khomenko et al., 2022	Europe (724)	Local administrative boundaries, with >50,000 inhabitants (European Commission's Joint Research Centre)	Urban Audit (Eurostat ^d)	High noise annoyance IHD (rate per 100,000 and YLL)	Guski et al., 2017 Eurostat (European Commission, 2019) (City-level)	2015	Road traffic noise (250m)	Environmental Noise Directive (European Commission, 2002)	IHD-1.05 (0.97–1.13) per 10 dB increase	van Kempen et al., 2018	Country-specific prediction models (250m ²) using ordered logistic regression for aggregated data.	53 dB

Abbreviations: Years of life lost (YLL); Effects of low-level air pollution: a study in Europe (ELAPSE); Land Use Regression (LUR); Screening for High Emission Reduction Potentials for Air Quality (SHERPA); European Monitoring and Evaluation Programme for Transboundary Long-Range Transported Air Pollutants Meteorological Synthesizing Centre-West (EMEP MSC-W); Ischaemic heart disease (IHD); Chronic obstructive pulmonary disorder (COPD); Global Health Data Exchange (GHDX); Cardiovascular disease (CVD); Disability-adjusted life years (DALYs); Global Burden of Disease Study (GBD); State Environmental Protection Administration of China (SEPA); Total suspended particles (TSP); Normalised differential vegetation index (NDVI); Terra Moderate Resolution Imaging Spectroradiometer (MODIS) Vegetation Indices (MOD13Q1); Urban heat island (UHI).

^a Spatial scale denotes the finest level of analysed health data. Resolution scale denotes the grid-cell level the exposures were estimated at, when reported.

^b ERF source used to calculate relative risk.

^c Age-specific RR calculated for each grid cell PM_{2.5} concentration not reported, available from the authors upon request.

^d Average taken from 20-year time series and therefore was not a trend analysis.

confounding variables, population density (−0.15, −0.17), physical inactivity (0.65, 0.67), median age (−0.11, −0.11), and income (−0.98, −0.95) were significantly associated with obesity (reported β coefficients are for greenness and tree cover, respectively). Whilst median income (−0.85, −0.86) and physical inactivity (0.21, 0.2) were significantly associated with poor mental health (Browning and Rigolon, 2018).

Although evidence was mixed, urban form characteristics of denser housing (Olsen et al., 2019), higher population density (McDonald et al., 2023), and more compact cities (Anderson et al., 2022) generally showed a negative association with green space availability. Aiming to advance predictions of the benefits of increasing green space, Marando et al. developed a model that simulated the microclimate regulation of urban green infrastructure across European cities (Marando et al., 2022). To lower temperatures by 1 °C in urban areas, a minimum tree cover of 16% was required. Of the Functional Urban Areas (FUAs) studied in Europe, 32% (192 FUAs) had tree cover below 16%. A global review by McDonald et al. explored how urban areas can achieve both population density and green space and found a 10% increase in density was associated with 2.9% decline in tree cover (Marando et al., 2022). Interestingly, the reported negative correlation was weakest when explored at neighbourhood level compared to city-level, suggesting some neighbourhoods achieved more tree canopy than was expected based on population density. Supportive findings by Anderson et al. observed variation between cities in the magnitude of cooling benefits from green space and attributed this to different distributions of green space within cities (Anderson et al., 2022). Cities with the same availability of green space (20%) but different levels of proximity experienced varying cooling effects during a heat wave, 55% of one city's population was estimated to benefit in contrast to 16% of another city's population (Anderson et al., 2022).

3.2.4. Urban form and transport and mobility

Bassolas et al. developed a metric that quantifies the hierarchical organisation of urban mobility, considered a proxy for urban inhabitants' needs being met (Bassolas et al., 2019) (Table A1 in Appendix). Weekly trip flow information of 300 million people in 301 global cities was aggregated into weighted networks to identify hotspots of activity at spatial resolution of ~1.27 km (The World Bank) and city-level. The varied spatial distribution patterns of hotspots captured differences in city organisation, permitting inferences of the effects of urban structure on transportation (mode share), pollutant emissions, and health outcomes (ischaemic stroke mortality and fatal traffic injuries). Greater urban mobility was attributed to more population mixing (Pearson's coefficient (R_P²) = 0.21, Spearman's coefficient (R_S²) = 0.24), extensive use of public transportation (R_P² = 0.45, R_S² = 0.39), higher levels of walkability (R_P² = 0.47, R_S² = 0.58), and better health outcomes (ischaemic stroke mortality rate per 100,000 inhabitants: R_P² = 0.31, R_S² = 0.26, fatal traffic injuries: R_P² = 0.34 and R_S² = 0.33). Another study that applied advanced techniques of remote sensing and global geospatial data identified nine global city types by modularity analysis (Thompson et al., 2020). The poorest performing cities for road traffic injuries were characterised by sparse and irregular shapes with large blocks, whereas the best performing city types were characterised by high rates of public transportation. Road traffic injury burden of 9.6 million DALYs were attributed to suboptimal urban design (Thompson et al., 2020).

3.3. Health impact assessment

Of the 45 urban environmental health studies, 25 applied a HIA methodology. All the HIAs followed a comparative risk assessment (CRA) approach, with all but one HIA (Massetot et al., 2023) assessing the potential health impacts under an alternative scenario (i.e., counterfactual) (Mueller et al., 2023). To effectively examine the different HIA methodologies employed, this section is structured as follows:

environmental exposures, population and health data, exposure response functions (ERFs) and counterfactual scenarios, and summary of findings.

3.3.1. Environmental exposures

Almost 85% of the HIAs (21) analysed the health impacts from air pollution. Of these HIAs, eight obtained pollution exposure data from the common data repository of China National Environmental Monitoring Centre (CNEMC), two utilised a dataset produced by Anenberg et al. (2022), and the remainder obtained estimates from emission inventories (Khomenko et al., 2023; Guan et al., 2021a; Anenberg et al., 2019a; Diao et al., 2020; Han et al., 2022; Southerland et al., 2022; Zhang et al., 2008) or from air pollution models (e.g., land use regression models, EMEP MSC-W chemical transport model, and SHERPA tool) (Khomenko et al., 2021; Anenberg et al., 2019b; Maji et al., 2017; Malashock et al., 2022a) (Table 4). The majority of HIAs that focused on air pollution analysed PM_{2.5} as the environmental exposure (14, ~56%), followed by ozone (8, ~32%), NO₂ (7, 28%) and particulate matter diameter 10 µm (PM₁₀) (2, 8%) with one study assessing carbon dioxide (CO₂) (Anenberg et al., 2019b) and one sulphur dioxide (SO₂) and total suspended particles (TSP) (Mead and Brajer, 2006). Of the 25 HIAs, eight (32%) assessed temporal trends in air pollution, the longest trend assessed global NO₂-attributable paediatric asthma incidence across 29 years (Anenberg et al., 2022).

Of the four HIAs that analysed alternative environmental exposures, two assessed temperature health impacts (Peters et al., 2021; China National Environmental Monitoring Centre, 2020), obtaining temperature records from ERA5-Land dataset (100 m²) (Peters et al., 2021) and Copernicus UrbClim model application (100 m²) (China National Environmental Monitoring Centre, 2020); one assessed green space (Ortigoza et al., 2021) by normalised differential vegetation index (NDVI) and percentage of green area (%GA), obtained from the US Geological Survey (Stanaway et al., 2017) and European Urban Atlas (Copernicus. Urban Atlas, 2012, 2012b) (250 m²); and one estimated the impact of road traffic noise (Khomenko et al., 2022). Of the strategic noise maps acquired from the Environmental Noise Directive and local sources ~83% were considered low or moderate quality. Masselot et al. was the only HIA to analyse both extreme heat and extreme cold (Zanaga et al., 2021).

3.3.2. Population and health data

Similar city population data sources were applied based on the country HIAs were conducted in. For HIAs conducted in China, the National Bureau of Statistics of China was a common population data depository; all HIAs conducted in Europe (6, 24%) utilised the Urban Audit, whilst Global HIAs obtained population estimates from European Commission's Joint Research Centre or the Centre for International Earth Science Information Network (CIESIN) (Table 4). Health data were generally obtained at national or provincial-level and applied to city-level; two HIAs in China (Han et al., 2022; Mead and Brajer, 2006) and all HIAs conducted in Europe utilised city-level health data.

A diverse range of health outcomes were analysed, with each HIA examining between one and 24 health outcomes (Table 4). Mortality outcomes were a key focus, encompassing categories of all-cause mortality (14, 56%), cause-specific mortality (8, 32%), natural-cause mortality (3, 12%), and specific morbidity-related mortality (6, 24%). Mortality estimates mostly obtained from the Global Burden of Disease study (Institute for Health Metrics and Evaluation). Units ranged from total death counts, mortality rate per 100,000, DALYs and Years of Life Lost. Beyond morbidity and mortality, additional health outcomes included attributable hospital admissions, symptom onset, and high noise annoyance (Zhang et al., 2008; Khomenko et al., 2022). Notably, the majority of HIAs assessed health impacts in adults. Only two HIAs (8%) assessed health outcomes in children, focusing on premature paediatric mortality (Anenberg et al., 2022) and asthma attack, respiratory symptoms, and bronchodilator usage (Maji et al., 2017).

3.3.3. Exposure response functions and counterfactual scenarios

The most common sources of ERF were from epidemiological literature. Two HIAs obtained ERF estimates from local cohort studies, whilst one HIA estimated ERFs by atmospheric modelling with integrated risk function based on six meta-analyses (Southerland et al., 2022). Only one HIA developed their own ERFs (Masselot et al., 2023), and these were applied in another HIA to estimate UHI impacts (Iungman et al., 2023). Masselot et al. employed a three-stage modelling framework that applied daily time series temperature and mortality data, age-specific mortality, and composite indices of vulnerability to produce age- and city-specific ERFs (Masselot et al., 2023). The composite index of vulnerability was developed from distributed lag non-linear and meta-regression models and incorporated city size, proximity to green and blue space, and SE inequalities (Masselot et al., 2023). In general, ERFs were applied homogeneously to the adult study population. Exceptions included acute lower respiratory infection-specific ERF to infants under five years (Maji et al., 2017), city-specific and age group-specific ERFs for temperature (Iungman et al., 2023; Masselot et al., 2023), and morbidity- and health endpoint-specific ERFs (Maji et al., 2017, 2018; Diao et al., 2020; Zhang et al., 2008). There was variation in counterfactuals applied. Of the 13 HIAs (25%) that analysed health risk of PM_{2.5} exposure, five applied the same counterfactual 10 µg/m³ based on the 2005 WHO guideline, whilst three applied the 2021 guideline of 5 µg/m³ (Anenberg et al., 2019a; Han et al., 2022; Southerland et al., 2022). For air pollution, counterfactuals ranged: for PM_{2.5} 2.4–35 µg/m³^{126,139}; ozone 54–160 µg/m³^{139,140}; NO₂ ~3.78–80 µg/m³ and PM₁₀ 5.8–40 µg/m³ (Zhang et al., 2008; Maji et al., 2017). Two studies applied Chinese ambient air quality standards (CAAQS) as counterfactual scenarios (Zhang et al., 2008; Mead and Brajer, 2006), whereas Khomenko et al.'s study was the only one to apply the lowest measured concentration in the dataset as an additional counterfactual concentration (Khomenko et al., 2021). Barboza et al. based counterfactuals on the WHO recommendation of universal access to green space (i.e., equal opportunity to access) within 300 m of residence, applying counterfactuals of 25% GA within 300m of residence and a target NDVI modelled for each city (Barboza et al., 2021). Another HIA based in Europe estimated the mortality burden attributable to UHI by applying city-specific counterfactuals of exposure level scenarios without an UHI effect and estimated the impact on mortality by increasing tree coverage to 25%, 30%, and 40% (Anenberg et al., 2019b). The only study to focus on road traffic noise health impacts applied WHO recommendation of 53 dB, which remains the current guideline (Khomenko et al., 2022).

3.3.4. Summary of findings

Global HIAs consistently reported cities in southeast Asian countries to experience the greatest pollutant concentrations and attributable health impacts worldwide (Southerland et al., 2022; Anenberg et al., 2019b; Malashock et al., 2022b; Song et al., 2023). Inconsistent findings from HIAs conducted across the same years 2015 and 2020 in China reported ozone-related impacts increased by ~95% (5.05 × 10⁶ DALYs) and 96% (7.64 × 10⁵ DALYs) for all-cause and respiratory mortality (Guan et al., 2021b), respectively, in contrast to ozone-attributable impacts reported to increase by 17% for all-cause mortality (133,415 deaths in 2015 to 156,173 deaths in 2020) and 17% for respiratory mortality (28,614 deaths in 2015 to 33,456 deaths in 2020). For NO₂, a global HIA reported highest NO₂-attributable deaths in South Asia (75, 397 deaths) and Eastern Europe (46,840 deaths) (Song et al., 2023). Whereas within Europe, Khomenko et al. reported the highest NO₂ mortality burden was in Western and Southern European capital cities and applied local-level mortality rates; highest burden cities were Madrid (Spain), Antwerp (Belgium), and Turin (Italy) (Khomenko et al., 2021).

Temporal trend HIAs revealed declining trends in PM_{2.5} concentrations and attributable mortality in China and globally (Anenberg et al., 2019a; Han et al., 2022). Southerland et al. reported the largest absolute

decrease in mean urban population-weighted PM_{2.5} concentration between 2000 and 2019 was in Africa, decreasing by 18% (Southerland et al., 2022). However, in certain regions, such as Luanda (Angola), there was an increase in PM_{2.5} concentrations and directional trends did not consistently align with trends in attributable mortality rates (an observation potentially explained by reported population growth). Another global temporal HIA covering 2000–2019 reported South and East Asia accounted for the highest proportion of global population ozone-attributable mortality in 2019, followed by Eastern Europe. However, this HIA reported divergent trends within South and East Asia; population-weighted ozone concentrations and mortality rates increased across all cities in South Asia, and decreased across all cities in East Asia (Malashock et al., 2022b).

Additional insights from temporal trend analyses were the contribution of HIA parameters to health impact estimates. For ozone-attributed mortality, key global drivers were ozone concentrations and population, and for a few regions changes in baseline disease rates (Malashock et al., 2022b). For PM_{2.5}-attributed mortality, changes in population growth and population ageing were the primary drivers in all regions (Southerland et al., 2022). For specific cities across Africa, the Eastern Mediterranean, and Southeast Asia, changes in baseline disease rates had the largest impact. Conversely, in the Western Pacific, the Americas, and Europe, reductions in PM_{2.5} concentrations outweighed the influence of baseline disease rates (Southerland et al., 2022).

In addition to regional variation in exposure attributable health burden, there was heterogeneity among cities and age groups. In Europe, cities in Northern Italy were amongst cities with the highest mortality burden despite Italy not placing highest for PM_{2.5}-attributed mortality burden in country-level estimates (Khomeiko et al., 2021). Similarly in Europe, Barboza et al. reported 42,698 and 17,947 annual deaths could be prevented by increasing NDVI and %GA, respectively, and found unequal distribution of NDVI and %GA among and within cities (Barboza et al., 2021). The only HIA to assess the impacts of non-optimal temperatures reported large variability in vulnerability across Europe (Masselot et al., 2023). The highest vulnerability was found in eastern European cities during extreme cold and heat and in age groups of over 85 years, which contributed over 60% to the total mortality burden. Annual excess deaths of 203,620 deaths (129 per 100,000 person years) were attributed to cold temperatures and 20,173 annual excess deaths (13 per 100,000 person years) attributed to heat. Iungman et al. found that increasing tree coverage to 30% can reduce city temperatures by 0.4 °C and prevent almost 40% (2644 premature deaths) of 6700 premature UHI-attributable deaths (Iungman et al., 2023). The only study to examine the effects of noise on health reported 11 million adults, of the estimated 60 million exposed to road traffic noise, to experience significant annoyance and 3608 IHD-deaths could have been prevented if compliance with WHO recommendations were achieved (Khomeiko et al., 2022). City comparative analysis was not possible due to inconsistencies in noise mapping methods.

3.4. Indicators

Identified indicators covered the key themes of this review: urban form, air pollution, temperature, green space, noise, and transport and mobility; in addition to climate change mitigation, which encompassed indicators of greenhouse gas emissions and climate change impact on trees. The indicators identified and methods employed, in addition to geographical coverage, spatial resolution, and data sources, are detailed in Table A1 of the Appendix. There was heterogeneity in spatial resolution of indicators; the greatest variation was amongst air pollution indicators, which ranged from 0.01° resolution to the coarsest resolution of NUTS3 level, a territorial unit defined by the European Commission Urban Audit that typically encompasses districts or boroughs (Eurostat Archive) (Table A1).

As part of a *Lancet* series on urban design, transport and health (The Lancet, 2022), Boeing et al. developed an open-source framework with

urban spatial indicators for measuring walkability and public transport access (Boeing et al., 2022). A total of 25 global cities were compared to elucidate the optimal urban design for promoting active travel (Giles-Corti et al., 2016). Applying the developed walkability index, Boeing et al. found compact cities had better walkability, whereas the worst performing cities for active travel were concentrated in more sprawled cities in high-income countries (HIC), such as Australia and the United States, consistent with previous findings (Behnisch et al., 2022; Lowe et al., 2022). To add to the utility of these indicators, Cerin et al. sought to provide evidence-informed thresholds (Cerin et al., 2022). To meet the physical activity criteria of urban inhabitants having at least 80% probability of engaging in walking for transport, and WHO's target of at least 15% relative reduction in insufficient physical activity through walking (World Health Organisation, 2020), neighbourhood targets associated with meeting one or both criteria were identified as: 5700 people per km (The World Bank), 100 intersections per km (The World Bank), and 25 public transport stops per km (The World Bank). Curvilinear associations of population, street intersection, and public transport densities with walking revealed less than a quarter of the studied population lived in neighbourhoods that reached these thresholds, with observed between-city differences; cities in Latin American upper-middle-income countries performed better than those in HIC. Another transport and mobility indicator that aimed to measure how conducive the urban environment is to active transport was the extent of bicycle network in a city (Akande et al., 2019). Akande et al. utilised the UNECE-ITU Smart Sustainable Cities Framework to rank 28 European capital cities based on 32 sustainability indicators covering the thematic areas of economy, environment, and society and culture (UNECE, 2017). Berlin (Germany) was ranked the most smart and sustainable city; indicators of bicycle network, wastewater treatment, and e-commerce had the greatest impact on ranking. Conversely, Sofia (Bulgaria) and Bucharest (Romania) were the lowest ranked cities, rankings were most influenced by indicators PM₁₀ emissions and protected terrestrial area (Table A1). Other novel indicators of urban form included access to urban services and amenities, considered proxies for opportunities and living standards within cities (Mackres et al., 2023; Boeing et al., 2022).

Climate change mitigation indicators have the potential to advance understanding of how cities contribute to climate change, forecast impacts, and potential mitigation strategies. One indicator depicted the percentage change in greenhouse gas emissions between 2000 and 2020 at city-level, disaggregated by pollutant and sector (e.g., agriculture from livestock, soils, and waste burning, industry, residential, commercial, and off- and on-road transportation) (Mackres et al., 2023); in addition to a 20-year global warming potential and total emission summaries for 2000 and 2020 (Table A1). Pertinent to climate change urban mitigation strategies, the average annual greenhouse gas net flux from trees (per hectare of city area) was provided for a 21-year period, 2000 to 2021 (Table A1). This is complimented by an indicator of the same global coverage, which estimated the percentage of urban built-up land absent of tree cover (Mackres et al., 2023). Related temperature indicators included the percentage of built-up land with low surface reflectivity (Mackres et al., 2023). This enables identification of areas within a city that exhibit low solar reflectivity and thereby could derive significant benefit from the implementation of tree planting and green spaces.

Departing from commonly applied green space indicators that measure NDVI and %GA, novel methods for analysing green space included accessibility, quality, level of urban biodiversity, and the relation between green space and inequality (Table A1). Battiston & Schifanella developed a composite index for green space accessibility and exposed variation between-city levels; cities in Europe and Australia-Oceania had higher green space accessibility compared to regions in low- and middle-income countries and North America (Battiston and Schifanella, 2023). The index' sensitivity to parameterisation was evident from adjustment of metrics, such as level of inequality (defined by the GINI coefficient), resulting in different area rankings of green

space accessibility. Complimentary work has aimed to quantify green space accessibility based on quality, defined as “high-amenity nature” (Daams and Veneri, 2017). Ranking cities by amenity of accessible nature revealed higher population densities, although living generally further from nature, live closer to high-amenity nature compared to residents of lower urban population densities. Further advances for analysing green space were illustrated by Stowell et al. who applied cloud computing technology and analysis of remote sensing data to produce an urban greenness indicator dataset (measured by population-weighted peak and annual mean NDVI). Although an NDVI metric is not novel, 1000 global cities were classified based on level of greenness, climate zone, and HDI for the years of 2010, 2015, and 2020, which allows for temporal tracking of urban greenness— an attribute not available in other reviewed indicators (Stowell et al., 2023) (Table A1).

4. Discussion

The purpose of this review was to synthesise evidence from large-scale urban studies that focused on the relation between urban structures, environmental exposures, and health and to identify future opportunities for urban health research. To achieve this, the research questions we sought to address were: what methodologies were applied in urban form, transport and mobility, and urban environmental health studies from 2003 to 2023? What are novel methods and indicators within urban environmental health research? What knowledge gaps necessitate further exploration?

Key findings from this review confirm the complex, intricate relation between the urban environment and health. This is evidenced from the discordant impacts from urban form variables on exposures and health. For example, compactness (Prieto-Curiel et al., 2023; Taubenböck et al., 2020), high population density (Ortigoza et al., 2021; Bilal et al., 2021; Prieto-Curiel et al., 2017, 2023), green space (Browning and Rigolon, 2018; Rezaei and Millard-Ball, 2023; Avila-Palencia et al., 2022b; Barboza et al., 2021), and extensive public transportation and active travel infrastructure (Ortigoza et al., 2021; Avila-Palencia et al., 2022a; Bassolas et al., 2019; Cerin et al., 2022) were found to have a multitude of benefits, which promote health and well-being (Bassolas et al., 2019; Boeing et al., 2022; Cerin et al., 2022). Conversely, increasing density and compactness were associated with the trade-offs of reduced green space (Anderson et al., 2022; McDonald et al., 2023), accentuated UHI (Jungman et al., 2023; Zhou et al., 2017), and higher pollutant concentrations and exposure from congestion (Gouveia et al., 2021; Kephart et al., 2023). Urban sprawl and fragmented city shapes were generally reported to have negative implications for city liveability (Taubenböck et al., 2020) and health (Bilal et al., 2021; Avila-Palencia et al., 2022a). This pertains to the ‘15-min city’ model, wherein all essential amenities for the urban residents’ needs, such as health, socialisation and culture, are accessible by walking or cycling within a 15-min radius (Allam et al., 2022). The strong correlation between urban sprawl and HDI could indicate sprawl has positive ramifications, owed to HDI incorporating life expectancy, educational attainment, and gross national income per capita (Behnisch et al., 2022). Urban scaling laws offer a partial explanation, as linear urban scaling delineates that larger cities generate higher wages (Rybski et al., 2019), consistent with findings of city size being the most influencing factor for urban sprawl (Prieto-Curiel et al., 2023). Spatial analysis of urban form characteristics by Prieto-Curiel et al. demonstrated concomitant analysis is critical for understanding how urban shape and structures affect the functional and social aspects of urban living (Prieto-Curiel et al., 2017).

An important inference from reviewed literature is the distinction between exposure and vulnerability, as certain less-exposed groups may have heightened vulnerability to the exposure under study. For example, sophisticated methods employed by Masselot et al. found the highest vulnerability to extreme cold and heat was in age groups of over 85 years (Masselot et al., 2023). Differential risk levels from extreme temperatures based on gender have been illustrated elsewhere, women aged 65

years and above and men below 65 years showed the highest vulnerability to hot temperatures (Ballester et al., 2023). In Europe, groups of lower SES had lower MMT (Krummenauer et al., 2019), whilst in Latin America higher levels of poverty and income inequality were associated with all-age MMT and higher cold MMT (Bakhtsiyarava et al., 2023). Inequality-driven variation in exposure levels was also present; reduced access to green space and therefore increased PM_{2.5}-exposure was reported in lower income groups (Rezaei and Millard-Ball, 2023).

4.1. What methodologies were applied in urban form, transport and mobility, and urban environmental health studies from 2003 to 2023?

There was heterogeneity across studies in methodologies, indicators, and city boundaries (Tables 3 and 4). Sub-city units can vary in size and composition, and therefore, the boundaries of urban agglomerations can have a considerable effect on results, creating a potential bias towards larger cities (Anderson et al., 2022). Harmonised city definitions are a key challenge and may have contributed to contrasting results. To achieve cooling effects of urban green in Europe, tree cover of at least 16% was estimated to achieve a reduction of 1 °C (Marando et al., 2022), whilst an HIA study estimated 30% tree cover would be required to reduce temperatures by 0.4 °C (Jungman et al., 2023). Jungman et al. employed a city-level model (Jungman et al., 2023), whilst Marando et al. utilised FUAs (Marando et al., 2022), which encompass the surrounding community zone and suburban areas (Eurostat[®]). Approaches to defining cities of the reviewed studies were based upon administrative boundaries (Khomenko et al., 2021), functional definitions that rely on travel patterns and economic connections (Marando et al., 2022), or morphological approaches that create shapes based on the extent of built-up or urbanised areas (Rezaei and Millard-Ball, 2023); the choice of definition typically depends upon research objectives. An operational city definition independent of context specificity would improve meaningful comparisons and transparency among studies.

The prevailing study design applied was cross-sectional or ecological (Table 3), which reflects a wider challenge in the field of requiring longitudinal studies and thus more robust causal inferences of the relation between urban design and health (Fazeli Dehkordi et al., 2022). This has further implications that the exposure-response relationships may be limited and therefore captured in analyses. For example, the link between urban land use, transport and mortality, and health is conceptually well understood; however, it lacks comprehensive quantitative evidence (Tonne et al., 2021).

In addition, the exposures under study may not accurately represent population exposure. In urban environmental health studies focused on green space, proximity was the primary exposure variable analysed. Exploration of the frequency (Bao et al., 2023) that urban residents visit green space, potential variation in access between demographic sub-groups (Bao et al., 2023), and the quality and amenity can augment the understanding of population exposure and attributable health impacts. Research examining spatial inequalities in quality and accessibility of green space consistently report residents of more deprived neighbourhoods experience longer travel time to access green areas (Phillips et al., 2022; Hoffmann et al., 2017). In Brussels (Belgium), area-based deprivation levels were associated with reduced satisfaction and authors identified factors that influence the use of green space, such as positive attributes of tranquillity and cleanliness and negative attributes of noise and lack of facilities (Phillips et al., 2022). Further, none of the reviewed air pollutant studies explored indoor air pollution. Long-term exposure to indoor air pollutants can pose significant risk to human health (Van Tran et al., 2020). A meta-analysis of burden of disease studies attributable to indoor air pollutants in China, found 9.5% more DALYs were attributable to indoor air pollutants compared to outdoor pollutants in 2017 (Liu et al., 2023). Given that people spend the majority of their time indoors, incorporation of indoor pollutant exposure estimates would ensure predicted health impacts are comprehensive and effectively advance the understanding of the magnitude of this exposure

pathway. Novel materials for sensors, indoor air pollution-monitoring systems, and smart homes show promise for advancing exposure and impact estimations of indoor air quality (Van Tran et al., 2020).

In comparison to the other study designs employed, the HIA methodology can present distinct advantages; however, equally have distinct challenges. Within China, divergent estimates of ozone-attributable impacts for all-cause and respiratory mortality highlight the sensitivity of methodological choices (Guan et al., 2021b; Zhang et al., 2022). These respective studies applied the largest difference in counterfactuals of pollutant HIAs reviewed; Guan et al. (2021b) estimated impacts relative to 160 $\mu\text{g}/\text{m}^3$ whereas Zhang et al. (2022) applied counterfactual of 54 $\mu\text{g}/\text{m}^3$. This may partially explain varied findings and highlights the significance of counterfactual scenario choices, in addition to the difficulty in study comparisons when different health outcomes are assessed (e.g., DALYs vs. deaths). Further, models used to calculate pollutant exposure levels are generally built using data representative of the average exposure and thus extremes in concentration response relationships are poorly understood. Investigation on the significance and choice of counterfactual scenarios was beyond the scope of this review; however, it highlights an important conjecture when conducting HIAs and interpreting results.

Additional insights from temporal trend HIAs were the ability to track impact over time and identify impact drivers of policies and exposure level changes. This can introduce the methodological challenge of the sensitivity ascribed to chosen years. Of the eight temporal studies, three included the year 2020 and thus the COVID-19 pandemic is likely to have influenced exposure levels and impact estimates (Guan et al., 2021b, 2022b; Zhang et al., 2022). Whilst estimates of temperature-attributed health impact will be largely affected by a particularly hot year being included in analyses. Advances in available indicators that permit temporal tracking will improve the accuracy of temporal estimates and help mitigate this constraint. The only identified indicator that included temporal tracking was for green space availability, which may be particularly useful in understanding climate change resilience of different urban green types (Stowell et al., 2023).

4.2. What are novel methods and indicators within urban environmental health research?

The importance of studying local variance of environmental exposures and health impacts was illustrated and new methods and indicators show promise to this advancement. African cities with the same availability of green space were found to experience varying cooling effects during heat waves (Anderson et al., 2022). This was ascribed to varied distributions of green space within cities, suggesting availability is not the same as proximity and quality. This inference was corroborated by Barboza et al. whose sensitivity analyses suggested population distribution within cities influenced local differences of green space-attributable health impacts (Barboza et al., 2021). To achieve a balance of dense and green cities, future research analysing the cooling effects of urban tree cover should consider the effects of climate change and urban green resilience (Esperon-Rodriguez et al., 2022). The greatest environmental benefits are considered to be provided by long-stature, mature trees and thus this is an important consideration for the time required and potential impact of climate change and UHI mitigation strategies (Esperon-Rodriguez et al., 2022). Novel green space indicators of green space quality (Daams and Veneri, 2017), level of amenity (Akande et al., 2019), and urban biodiversity (Mackres et al., 2023) offer to advance this understanding. The latter may improve understanding of the ecological quality and species-richness; greater biodiversity closer to residence requires large urban connected patches and offers positive benefits on mental health and well-being (Anderson et al., 2022).

The emergence of cutting-edge technologies (Son et al., 2023; Essamlali et al., 2024) and advances in remote sensing and geospatial data sources present significant opportunities to enhance the

comprehension of intricate urban health phenomena and the identification of key elements for sustainable urban design (Barboza et al., 2021; Fazeli Dehkordi et al., 2022). These advancements hold the potential to address challenges related to diverse urban form metrics and definitions by leveraging geospatial data sources. These sources can improve the accuracy of population-weighted averages for obtaining overall urban metrics or enable the disaggregation of cities into neighbourhoods, thus facilitating better harmonisation. A key challenge will be effective translation of vast quantities of remote sensing and other spatial data sources into interpretable evidence of the complex spatial interactions (Fazeli Dehkordi et al., 2022); however, deep learning algorithms offer a promising solution to this challenge, through techniques such as semantic segmentation (Jia et al., 2024).

Further applications of spatial data science and artificial-intelligent (AI)-driven tools for supporting sustainable urban development include agent-based modelling (ABM) (Motieyan and Mesgari, 2018) and machine learning algorithms (Son et al., 2023). Motieyan et al. utilised an ABM to simulate the implementation of superblocks, an urban model that prioritises public space for active transport and leisure and minimises motorised traffic (Nieuwenhuijsen et al., 2024). By incorporating individual “agents” diverse behavioural patterns of local citizens were simulated which enabled anticipation of public opinion and acceptance of superblock implementation. Machine learning algorithms are enhancing predictions of environmental exposures, through methods such as integration of urban morphology data (e.g., topography and building height) into air quality forecasts (Wang et al., 2024). Woo Oh et al. trained deep learning models using meteorological data and urban texture factors (e.g., surface albedo) to develop temporal- and spatial-UHI models (Oh et al., 2020). The temporal UHI model that quantified the number of UHI hours rather than intensity, was found to be a better predictor of seasonal UHI predictions and therefore improved estimations of attributable heat-related mortality (Oh et al., 2020). Future urban research is likely to combine and harmonise data from various scales and sources, and leverage Spatial Data Science and AI-driven technologies to gain a more comprehensive understanding of urban dynamics, challenges and solutions.

4.3. What knowledge gaps necessitate further exploration?

A minority of studies included SE and demographic variables in analyses; however, observations from those that did confirm social determinants are an important avenue of future urban environmental health research. This would advance understanding of whether distinct urban form types can mitigate inequalities. Further, investigating inequalities within cities is particularly important in light of the limited knowledge of vulnerability drivers responsible for across city variation. These differences can be important; for example, differences in air pollution-attributable health burden are mostly due to differential levels of pollutants and can partly be explained by the pollutant chemical compositions (Stafoggia et al., 2022), whereas for other drivers, such as temperature, differences can be due to the level of vulnerability and resilience of the population (Romero-Lankao et al., 2012).

The paucity of demographic and SE data available at local-level was a commonly cited reason for not examining between population-group differences. This dearth of data both impedes the identification of health disparities and undermines the formulation of targeted and effective public health strategies for vulnerable populations. This is reflected in the literature from the limited evidence on gender-specific outcomes from urban adaptation intervention (Solomon et al., 2021). Females have been shown to experience multiple barriers to public transportation accessibility and thus this may influence female commuting choices and in turn exposure levels (Mejía-Dorantes and Soto Villagrán, 2020). For HIAs, a methodological challenge central to the tendency of not stratifying estimates by gender and age is the lack of available sub-group ERFs. This reflects a gap in the underlying epidemiological evidence (Cohen Hubal et al., 2000). The lack of age-specific

ERFs, particularly for populations under 20 years, may also be a by-product of the overemphasis on PM_{2.5} and O₃ pollutants in the literature. PM_{2.5}- and O₃-related mortality impacts generally focus on the over 25-year-old population; however, in recent years more research has emerged for NO₂-related health outcomes in paediatric populations (Anenberg et al., 2022), (Achakulwisut et al., 2019).

4.4. Limitations of urban environmental health studies

The pathways covered in this review are not an exhaustive list and do not cover all pathways to health. Additional pathways that hold relevance include social exclusion (Glazener et al., 2021b), community severance (Glazener et al., 2021b), stress (Glazener et al., 2021b), and proximity to blue space (Smith et al., 2021). There was an evident paucity of research investigating health burden attributed to noise pollution. The only noise study analysed impacts from road traffic noise; however, aircraft, rail and construction noise also have considerable health impacts (European Environment Agency, 2020), (Mir et al., 2023). The household noise annoyance indicator may capture some of this exposure; however, the finest spatial resolution of NUTS3 restricts inferences for within city variability (Table A1). No studies incorporated climate change risk, which is a notable limitation for the HIAs that projected extreme heat and UHI.

The majority of studies applied regional-level estimates at city-level and assumed uniform distribution across cities, which discounts variability within and between cities. Commonly cited reasons for applying regional estimates were inconsistent data quality and availability at local-level and finer spatial resolutions (Anenberg et al., 2022; Guan et al., 2021a; Zhang et al., 2008); however, this can introduce the risk of uncertainty in local impact predictions. Approaches to mitigate this included extrapolating metrics from geographies with greater data coverage (Masselot et al., 2023; Song et al., 2023) or excluding geographies from analyses (Jungman et al., 2023). The latter pertains to the significant challenge of conducting HIAs in low- and middle-income countries (Thondoo et al., 2019). Few studies investigated within-city variation (Barboza et al., 2021; Prieto-Curiel et al., 2023; Taubenböck et al., 2020; Nguyen et al., 2019; Kephart et al., 2023); the extent of which was also subject to data availability and quality (Barboza et al., 2021). Ensuring fairness in data exploration and identification of local inequities necessitates robust and comprehensive datasets with uniform data collection at local-level. Central to this is collaboration across sectors, levels of government, and for researchers and practitioners to leverage open-data platforms (Boeing et al., 2022).

Applicable to all HIAs was the uncertainty attributed to ERFs and RRs. There was high variation in ERF data sources, which points to the general uncertainty surrounding the selection of the most accurate ERFs to apply (Table 4). For the majority of HIAs, the same ERFs were applied to the general population, which assumes equivalent risk. The paucity of sub-group ERFs that capture susceptibility merits that recommendations cannot be made for susceptible subpopulations.

4.5. Strengths and caveats of review

This was a scoping and not a formal systematic review, and therefore, aimed to provide a holistic overview of evidence from large-scale urban studies, rather than assess all evidence concerning a single relationship (e.g., air pollution and birth weight). Inclusion of additional health outcomes (e.g., mental health) in search terms may have identified further large-scale urban studies of relevance. Investigation of the interplay between urban environments and both established and emerging infectious diseases was beyond the scope of this review; however, these pathways have high relevance to the complex urban health ecosystem. Changes to land use, demographic shift patterns, and globalisation infrastructures have been identified as pivotal factors that influence infectious disease incidence and outbreak (Connolly et al., 2021). The COVID-19 pandemic illustrates the crucial role of

governments and policies in managing infectious disease outbreaks, and highlights the inevitable trade-offs and conflicts encountered in planning strategies (Agyapon-Ntra and McSharry, 2023). Enhancing understanding of the interconnection between urban form and infectious diseases holds significant prominence in both research and governmental priorities for urban and transport planning. The scope of exposures included in this review aligned with those of the UBDPolicy project (Urban Burden of Disease Policy); however, the caveat of additional pathways being excluded pertains to the broader challenge of prioritisation and resource constraints. Initiatives such as Urbanisation and Health Initiative (World Health Organisation) led by the WHO, and the Urban Health Collaborative (University) led by Drexel University, recognise the significance of investigating non-communicable and infectious diseases in tandem.

Strengths of this review include the expert consultation of relevant literature, which extended the scope of reviewed studies, and inclusion criterion of large-scale urban studies, which serves to increase the reliability and generalisability of results. Equally, this may have been a limitation as potential insights may have been missed from the 90-city inclusion criterion. Studies of fewer cities may have covered understudied regions and vulnerable populations. Not all geographical regions were covered (for example Australia and South Asia) and only English search terms were included in the literature search, exclusion of studies conducted in other languages may have contributed to the geographic distribution of studies and introduced bias in reported results. However, 22 studies were global in geographic coverage, this is considered a strength and may have mitigated potential exclusion bias. Further, PubMed was the sole electronic database articles were obtained from. This was due to PubMed's comprehensive coverage of health and biomedical research. Finally, examination of urban policies and affiliated impacts was beyond the scope of this review.

5. Conclusion and future perspectives

This scoping review aimed to synthesise evidence from large-scale urban studies to provide a state-of-the-art overview of the relation between urban structures, transport, environmental exposures, and health. The complexity of the urban ecosystem was evidenced and emphasises the need for a multi-faceted approach for elucidating the intricate urban environmental health pathways. Researchers should prioritise exploring associations at multiple spatial scales and resolutions, both within and between population groups. Identifying local disparities in exposure, vulnerability, and adaptation will require enhanced local-level data, open-source indicators, and shared consensus of best research practices. Advances in techniques, temporal trend analysis, and urban health and sustainability indicators show promising developments. To fully harness the potential of cities as key drivers of sustainable and healthy living, robust evidence should spearhead this change. Only then can policies and interventions realise the impact they set out to achieve.

CRedit authorship contribution statement

Georgia M.C. Dyer: Writing – review & editing, Writing – original draft, Conceptualization. **Sasha Khomenko:** Writing – review & editing, Supervision. **Deepti Adlakha:** Writing – review & editing. **Susan Anenberg:** Writing – review & editing. **Martin Behnisch:** Writing – review & editing. **Geoff Boeing:** Writing – review & editing. **Manuel Esperon-Rodriguez:** Writing – review & editing. **Antonio Gasparrini:** Writing – review & editing. **Haneen Khreis:** Writing – review & editing. **Michelle C. Kondo:** Writing – review & editing. **Pierre Masselot:** Writing – review & editing. **Robert I. McDonald:** Writing – review & editing. **Federica Montana:** Writing – review & editing. **Rich Mitchell:** Writing – review & editing. **Natalie Mueller:** Writing – review & editing. **M. Omar Nawaz:** Writing – review & editing. **Enrico Pisoni:** Writing – review & editing. **Rafael Prieto-Curiel:** Writing – review & editing. **Nazanin Rezaei:** Writing – review & editing. **Hannes**

Taubenböck: Writing – review & editing. **Cathryn Tonne:** Writing – review & editing. **Daniel Velázquez-Cortés:** Writing – review & editing. **Mark Nieuwenhuijsen:** Writing – review & editing, Supervision.

Declaration of competing interest

The authors declare that they have no known competing financial interests or personal relationships that could have appeared to influence the work reported in this paper.

Data availability

No data was used for the research described in the article.

Appendix

Table A1

Themes and indicators identified in this review.

Theme	Indicator	Description	Methods	Geographical coverage	Spatial resolution	Data Sources
Urban form	Recreational space per capita (Mackres et al., 2023)	The hectares of recreational space (open space for public use) per 1000 people.	Recreational space data retrieved from OSM. OSM tags are employed to retrieve polygons that delineate areas of parks, nature reserves, commons, playgrounds, pitches, tracks, protected areas and national parks. Population data retrieved from WorldPop. The total recreational area within a jurisdictional boundary was divided by the population within the boundary per 1000 individuals.	Global	–	WorldPop (Earth Engine Data Catalog, 2020a) (OpenStreetMap, 2022)
	Urban open space for public use (Mackres et al., 2023)	The percentage of built-up area that is open space for public use.	Recreational space data retrieved from OSM. OSM tags are employed to retrieve polygons that delineate areas of parks, nature reserves, commons, playgrounds, pitches, tracks, protected areas and national parks. Definition of urban open or non-open space for each 10m pixel of built land derived using the built-up from ESA. The ratio of masked pixels representing open space to the total count of masked pixels was used to calculate the percentage of built area designated to open space.	Global	10m	(OpenStreetMap, 2022) ESA WorldCover (Earth Engine Data Catalog, 2020b) Zanaga et al., 2021
	Proximity to public open space (Mackres et al., 2023)	The percentage of the population within walking distance (400m) of public open space.	Utilised the gridded population (100m). Retrieved open space polygons from OSM buffered to 400m to derive recreation catchment areas. The population residing within the recreation catchment areas was determined and converted into a percentage by dividing that value by the total population of the area of interest.	Global	400m (The World Bank)	WorldPop (Earth Engine Data Catalog, 2020a) (OpenStreetMap, 2022)
	Proximity to tree cover (Mackres et al., 2023)	The percentage of the population with an average tree cover of greater than 10 percent within walking distance (400 m) of their homes.	Utilised 10m resolution tree cover and the gridded population (100m). A neighbourhood reduction technique utilising a circular kernel with radius 400m was employed to the tree cover layer to determine the average percentage	Global	400m (The World Bank)	Mosaic Landscapes data set (Resource Watch) WorldPop (Earth Engine Data Catalog, 2020a)

(continued on next page)

Table A1 (continued)

Theme	Indicator	Description	Methods	Geographical coverage	Spatial resolution	Data Sources
			of tree cover within a 400m radius of each 10m pixel within the area of interest. The result is subsequently applied to filter the population layer, restricted to include 100m population pixels with an average tree cover of more than 10 percent within a 400m radius. The population within the 100m masked population layer is calculated and then converted to a percentage by dividing this figure by the total population of the area of interest.			
	Distance to local amenities (Boeing et al., 2022)	Percentage of population living within 500m of a fresh food market, a convenience store, and public transport.	Developed indicators for pedestrian network distance accessibility within a 500m radius, assessed for hexagonal grid cells and adjusted based on population percentage estimates.	Global (25 cities)	500m	Global Human Settlement Layer (European Commission's Joint Research Centre) Custom boundaries (see Appendix (Boeing et al., 2022)) (Open Street Map, 2017)
Air pollution	High pollution days (Mackres et al., 2023)	Annual number of days that air pollutants were above WHO air quality guidelines in 2020.	The extracted data combines satellite monitoring of pollutant concentrations with atmospheric modelling to estimate concentrations in close proximity to the Earth's surface. Reported the number of days in 2020 for each city that had near-surface concentrations of air pollutants that Exceeded WHO's guidelines for outdoor air pollutants (World Health Organization, 2021).	Global	80 km	CAMS Global Reanalysis EAC4 (Inness et al., 2019)
	Fine particulate matter exposure (Mackres et al., 2023)	Annual mean PM _{2.5} concentration as a percentage of WHO's air quality guideline for annual exposure.	Extracted data combines models of atmospheric mixing and chemistry with imagery analysis (from the Moderate Resolution Imaging Spectroradiometer and Sea-viewing Wide Field-of-view Sensor satellite instruments from NASA) to generate estimates of PM _{2.5} concentrations near the earth's surface, based on annual average concentrations for 2020. Each district's 2020 average PM _{2.5} concentration reported as a percentage of WHO's air quality guideline for annual exposure of 5 µg/m ³ The annual average is calculated over the area of the district. For example an average concentration of 15 µg/m ³ would be reported as 300 percent of the WHO guideline.	Global	0.01° (~1.1 km)	Atmospheric Composition Analysis Group (The World Bank, 2016)
	Long-term exposure to PM ₁₀ ²⁰⁰⁹	Number of days particulate matter PM ₁₀ concentrations exceed 50 µg/m ³ .	Calculated the sum of total days that PM ₁₀ concentrations exceeded 50 µg/m ³ for 2016.	Europe (28 cities)	NUTS3	Urban Audit (Eurostat ⁸)
	Annual NO ₂ exposure (Akande et al., 2019)	Annual average concentration of NO ₂ (µg/m ³)	Calculated the average annual concentration of NO ₂ for 2016.	Europe (28 cities)	NUTS3	Urban Audit (Eurostat ⁸)
Temperature	Built land without tree cover (Mackres et al., 2023)	The percentage of built land without tree cover.	Tree cover with resolution of 10m applied. Built-up land data was obtained from ESA WorldCover and used to mask the tree cover layer. Counted the number of built area pixels that also had tree cover, and the total number of pixels with built areas. These two values were divided to determine the percentage of built land covered	Global	10m	Mosaic Landscapes data set (Resource Watch) ESA WorldCover 2020 (Zanaga et al., 2021)

(continued on next page)

Table A1 (continued)

Theme	Indicator	Description	Methods	Geographical coverage	Spatial resolution	Data Sources
			by trees. The percentage of tree cover was inverted to calculate the percentage of built-up land that lacked tree cover.			
	Extreme heat hazard (Mackres et al., 2023)	The anticipated extreme heat event hazard (measured as the number of days above 35 °C in 2050) and the trend (indicated by the percentage change in the number of days exceeding 35 °C between 2020 and 2050).	Calculated the anticipated number of days with maximum near-surface air temperatures exceeding 35 °C, for 2020 and 2050. Subsequently subtracted the 2020 estimate from the 2050 and divided this difference by the 2020 estimate and multiplied the result by 100. The resultant value is calculated from a probability distribution model.	Global	0.25° pixel containing the city centroid	ERA5 global reanalysis (Hersbach et al., 2020) NEX-GDDP ensemble climate projections (Thrasher et al., 2012)
	Land surface temperature (Mackres et al., 2023)	Percentage of built-up land with a high LST during the hot season (greater than or equal to 3 °C above mean for built-up land).	LST calculated or each pixel in the area of interest using methods described elsewhere (Ermida et al., 2020) and Landsat imagery. Average LST is calculated from a compilation of Landsat images that are cloud-masked. Images span from 2013 to 2022 and are selected for each year from the month with the highest temperature recorded, as determined by the ERA5 daily aggregates (Hersbach et al., 2020). Average pixel LST were retrieved for built-up land cover areas, classified by the ESA WorldCover. Areas where the temperature exceeded the area average by 3 °C or more were excluded to determine the proportion of build-up areas with elevated LST.	Global	30m	Google Earth Engine (Ermida et al., 2020) ESA WorldCover 2020 (Zanaga et al., 2021)
	Surface reflectivity (Mackres et al., 2023)	The percentage of built-up land with low surface reflectivity.	Used pixel-wise albedo values derived from Sentinel-2 using the algorithms defined elsewhere (Bonafoni and Sekertekin, 2020). Annual mean albedo was calculated using cloud-free pixels from 2021. Values for built-up land cover were obtained by applying the built-up class from the ESA WorldCover dataset as a masking tool. Pixels with values lower than 0.2 were excluded to determine the proportion of built-up area with reduced surface reflectivity.	Global	10m	Google Earth Engine (Ermida et al., 2020) ESA WorldCover 2020 (Zanaga et al., 2021)
Green space	Open or green space (van Kempen et al., 2018)	Percentage of population living within 500m of a public open space	For data obtained from OSM, followed tagging guidelines and collaborator feedback to classify open or green spaces. Determined the percentage of population residing within 500m of a public open space.	Global (25 cities)	500m	Global Human Settlement Layer (China National Urban Air Quality Real-time Publishing Platform, 2020) OpenStreetMap (Mejía-Dorantes and Soto Villagrán, 2020)
	Urban greenness (Stowell et al., 2023)	Population-weighted peak and annual mean NDVI. Cities grouped by urban greenness indicator, HDI and climate region.	Cities were selected based on population size of 500,000 or more. Calculated population-weighted peak and annual mean NDVI. Classified cities based on the greenness indicator, climate zone, and level of development. Repeated analyses for 2010, 2015, and 2020 to facilitate the tracking of urban greenery over time. Data provided in tabular and graphical format.	Global (1000 cities)	1 km (The World Bank)	Landsat (United States Geological Survey) Global gridded population (Centre for International Earth Science Information Network (CIESIN), 2016) Global Human Settlement Urban Centre (European Commission's Joint Research Centre) Köppen-Geiger climate classification system (Köppen-Geiger climate classification system)

(continued on next page)

Table A1 (continued)

Theme	Indicator	Description	Methods	Geographical coverage	Spatial resolution	Data Sources
	Green space accessibility (Stowell et al., 2023)	Urban green space accessibility	For each identified city, constructed accessibility metrics by combining information on population estimates, spatial data on public green areas (utilised for calculating walking distances within two cells in the city) and land cover of green space. Calculated accessibility indices of minimum distance (to closest public green area), exposure (overall size of available public green space), per-person (m ² pre person of public green within walking distance from residential location). Evaluated the stability of each accessibility index through different parameterisations, including weighting by GINI coefficient; through application of Kendall rank correlation coefficient.	Global (1000 cities)	1 km (The World Bank)	United Nations (United Nations Development Program, 2022) Global gridded population (Centre for International Earth Science Information Network (CIESIN), 2016) Global Human Settlement Urban Centre (European Commission's Joint Research Centre) OpenStreetMap (OpenStreetMap, 2022) World Cover data (Agency TES, 2012) Open Source Routing Machine engine (Luxen and Vetter, 2011)
	Nature based well-being indicator (Daams and Veneri, 2017)	Approximates the 'actual' subjective quality of nature near people's homes.	High-amenity nature ³ identified by combining CORINE data on natural land use with clustered HSM data, on locations of attractive nature. Spatial cluster analysis conducted on HSM markers identifies natural areas that people have perceived as attractive. It produces a 250m ² grid covering the observed country. The density of HSM markers is measured for each individual grid within the larger grid. Calculates population-weighted mean distance to high-amenity nature.	Netherlands, Germany and Denmark	250m (The World Bank)	European Environmental Agency (CORINE land cover dataset 2006) (European Environment Agency, 2006) HSM database (Google Maps-based survey tool) (Brown and Kyttä, 2014)
	Percentage of amenity green space (Akande et al., 2019)	Share of land dedicated to green urban areas, sports, and leisure facilities	Calculated the percentage of a city's total land area dedicated to green spaces, sports, and leisure facilities.	Europe (28 cities)	NUTS3	Urban Audit (Eurostat ⁶)
	Biodiversity of built-up areas (Mackres et al., 2023)	The percentage of bird species in all areas that were also observed in built-up areas.	Calculated by dividing the number of bird species in built-up areas by the total number of bird species observed across all areas within the city. Built-up areas were delineated using data from the ESA. To estimate the saturation levels of species-area curves for the number of bird species, utilised research-grade observations of birds between 2016 and 2021. Calculations were conducted using the observations recorded on built-up land and all observations within city boundaries.	Global	–	ESA WorldCover 2020 (Zanaga et al., 2021) iNaturalist database (Global Biodiversity Information Faculty, 2022)
	Biodiversity of built-up areas (Mackres et al., 2023)	The percentage of KBA in built up areas.	Determined the build-up area within a KBA located within a city, and divided this by the total KBA area within the city and multiplied the result by 100.	Global	City-level	ESA WorldCover 2020 (Zanaga et al., 2021) Key Biodiversity Areas (BirdLife International, 2022)
	Proportion of urban terrestrial area (Akande et al., 2019)	The percentage of land in a city designated as protected natural areas.	Calculated the percentage of a city's total land area that is designated as protected natural areas.	Europe (28 cities)	NUTS3	Urban Audit (Eurostat ⁶)
Noise	Household noise annoyance	Proportion of population living in households considering that they suffer from noise	Calculated the percentage of the total population who reported being affected by noise.	Europe (28 cities)	NUTS3	Urban Audit (Eurostat ⁶)

(continued on next page)

Table A1 (continued)

Theme	Indicator	Description	Methods	Geographical coverage	Spatial resolution	Data Sources
Transport and mobility	(Akande et al., 2019) Urban mobility (Bassolas et al., 2019)	Quantifies the hierarchical organisation of urban mobility, considered a proxy for urban inhabitants' needs being met	Weekly trip flow information of 300 million people aggregated into weighted networks to identify hotspots of activity. Hotspots enabled analysis of hierarchical organisation in urban mobility and connection to city liveability. Spatial distribution patterns of hotspots capture differences in city organisation.	Global (174 cities) United States (127 cities)	~1.27 km (The World Bank) and City-level	(United States Census Bureau) (Google. Location history) Centers for Disease Control and Prevention (Centers for Disease Control and Prevention c.)
	Local walkability index (Boeing et al., 2022)	Combines population density, street intersection density, and daily living destinations in local neighbourhoods.	Calculated population density as the mean of the estimated population density within 1 km of local walkable catchments. Street intersections were calculated as the average of the estimated intersection density within 1 km of local walkable catchments. Daily living score was determined as the sum of binary access indicator scores to supermarkets, convenience stores, and public transport facilities, serving as a proxy for land use mix. Walkability index was calculated as the sum of z-scores, both within and between cities, for population density, intersection density, and daily living score.	Global (25 cities)	1 km (The World Bank)	Global Human Settlement Layer (European Commission's Joint Research Centre) Custom boundaries (see Appendix (Boeing et al., 2022)) (Open Street Map, 2017) General Transit Feed Specification data sources (see Appendix (Boeing et al., 2022)) World Bank (World Bank, 2020)
	Public transport access (Boeing et al., 2022)	Percentage of population living within 500m of a frequently serviced public transport stop.	Calculated the percentage of the population living within a 500m radius of any public transport stop.	Global (25 cities)	500m	Global Human Settlement Layer (European Commission's Joint Research Centre) Custom boundaries (see Appendix (Boeing et al., 2022)) (Open Street Map, 2017) General Transit Feed Specification data sources (see Appendix (Boeing et al., 2022)) Urban Audit (Eurostat [®])
Climate change mitigation	Length of bicycle network (Akande et al., 2019)	Length of dedicated cycle paths and lanes	Calculated the sum of lengths of dedicated bicycle paths.	Europe (28 cities)	NUTS3 ^b	
	Greenhouse gas emissions (Mackres et al., 2023)	The variation in annual greenhouse gas emissions (measured in CO ₂ equivalent [CO ₂ e]) from the city area between 2000 and 2020, expressed as a percentage and broken down by pollutant type and sector.	Sectors include various agricultural activities, power generation, industry, transportation, and waste management. Using Google Earth Engine, the emissions within city administrative boundaries were calculated, disaggregating the data annually by sector in tonnes/year for 2000 and 2020. All emissions were converted to CO ₂ equivalent based on 20-year global warming potentials for a standardised measurement. The final indicator presents the percentage change in CO ₂ equivalent emissions from 2000 to 2020.	Global	11 km	Google Earth Engine (Ermida et al., 2020) CAMS Global Anthropogenic Emissions (Granier et al., 2019)
	Greenhouse gas emissions (Akande et al., 2019)	Greenhouse gas emissions from transport (million tonnes)	Calculated the total greenhouse gases measured in equivalent carbon dioxide units, produced by transportation activities in a city over the course of a year.	Europe (28 cities)	NUTS3	Urban Audit (Eurostat [®])
	Climate change impact of trees	The average annual greenhouse gas net flux from trees (2001–	Calculated the average annual carbon flux for each area, by assigning a zero value to pixels	Global	30m	Google Earth Engine (Ermida et al., 2020)

(continued on next page)

Table A1 (continued)

Theme	Indicator	Description	Methods	Geographical coverage	Spatial resolution	Data Sources
	(Mackres et al., 2023)	21) per hectare (ha) of city area (megagrams [Mg] CO ₂ e/ha).	without carbon flux data. Mean carbon flux over the area was then calculated and divided by 21 to obtain an annual average for the 21-year period. This yielded an estimate of the average yearly net carbon flux per hectare for the area of interest. The entire geographical area, including non-forested regions, was employed for normalisation, with the total area serving as the denominator. Negative numbers indicate net greenhouse gas removals, whereas positive values denote net emissions.			Net Carbon Flux (Harris et al., 2021)

Abbreviations: OpenStreetMap (OSM); European Space Agency (ESA); Copernicus Atmosphere Monitoring (CAM); National Aeronautics and Space Administration (NASA); Land Surface Temperature (LST); Normalised Difference Vegetation Index (NDVI); Human Development Index (HDI); Hotspotmonitor (HSM); Key Biodiversity Indicator (KBA).

High amenity defined as one of the following: ecosystem services (ESS), quality of cultural ESS (aesthetics), natural land uses.

NUTS3: corresponds to small regions or local administrative units that include cities or urban areas (Guski et al., 2017).

References

- Abbfafati, C., Abbas, K.M., Abbasi-Kangevari, M., Abd-Allah, F., Abdelalim, A., Abdollahi, M., et al., 2020. Global burden of 369 diseases and injuries in 204 countries and territories, 1990–2019: a systematic analysis for the Global Burden of Disease Study 2019. *Lancet*. 396 (10258), 1204–1222.
- Achakulwisut, P., Brauer, M., Hystad, P., Anenberg, S.C., 2019. Global, national, and urban burdens of paediatric asthma incidence attributable to ambient NO₂ pollution: estimates from global datasets. *Lancet Planet Heal* [Internet] 3 (4), e166–e178. [https://doi.org/10.1016/S2542-5196\(19\)30046-4](https://doi.org/10.1016/S2542-5196(19)30046-4).
- Agency TES, 2012. Sentinel 2 [Internet]. https://www.esa.int/Space_in_Member_States/Spain/SENTINEL_2.
- Agyapon-Ntra, K., McSharry, P.E., 2023. A global analysis of the effectiveness of policy responses to COVID-19. *Sci Rep* [Internet] 13 (1), 1–15. <https://doi.org/10.1038/s41598-023-31709-2>.
- Akande, A., Cabral, P., Gomes, P., Casteleyn, S., 2019. The Lisbon ranking for smart sustainable cities in Europe. *Sustain. Cities Soc.* 475–487, 44(April 2018).
- Alahmad, B., Khraishah, H., Royé, D., Vicedo-Cabrera, A.M., Guo, Y., Papatheodorou, S. I., et al., 2023. Associations between extreme temperatures and cardiovascular cause-specific mortality: results from 27 countries. *Circulation* 147 (1), 35–46.
- Allam, Z., Bibri, S.E., Chabaud, D., Moreno, C., 2022. The ‘15-Minute City’ concept can shape a net-zero urban future. *Humanit Soc Sci Commun* 9 (1), 1–5.
- Almeida, D.P., Alberto, K.C., Mendes, L.L., 2021. Neighborhood environment walkability scale: a scoping review. *J Transp Heal* 23 (August 2020), 101261. <https://doi.org/10.1016/j.jth.2021.101261> [Internet].
- Anderson, B., Patiño Quinchia, J.E., Prieto, Curiel R., 2022. Boosting African Cities’ Resilience to Climate Change : the Role of Green Spaces, vol. 37.
- Anenberg, S.C., Henze, D.K., Tinney, V., Kinney, P.L., Raich, W., Fann, N., et al., 2018. Estimates of the global burden of ambient PM_{2.5}, ozone, and NO₂ on asthma incidence and emergency room visits. *Environmental* 126 (2), 1–14.
- Anenberg, S.C., Miller, J., Henze, D.K., Minjares, R., Achakulwisut, P., 2019a. The global burden of transportation tailpipe emissions on air pollution-related mortality in 2010 and 2015. *Environ. Res. Lett.* 14 (9).
- Anenberg, S.C., Achakulwisut, P., Brauer, M., Moran, D., Apte, J.S., Henze, D.K., 2019b. Particulate matter-attributable mortality and relationships with carbon dioxide in 250 urban areas worldwide. *Sci Rep* [Internet] 9 (1), 1–6. <https://doi.org/10.1038/s41598-019-48057-9>.
- Anenberg, S.C., Moheggh, A., Goldberg, D.L., Kerr, G.H., Brauer, M., Burkart, K., et al., 2022. Long-term trends in urban NO₂ concentrations and associated paediatric asthma incidence: estimates from global datasets. *Lancet Planet Heal* [Internet] 6 (1), e49–e58. [https://doi.org/10.1016/S2542-5196\(21\)00255-2](https://doi.org/10.1016/S2542-5196(21)00255-2).
- Atkinson, R.W., Butland, B.K., Anderson, H.R., Maynard, R.L., 2018. Long-term concentrations of nitrogen dioxide and mortality. *Epidemiology* 29 (4), 460–472.
- Avila-Palencia, I., Rodríguez, D.A., Miranda, J.J., Moore, K., Gouveia, N., Moran, M.R., et al., 2022a. Associations of urban environment features with hypertension and blood pressure across 230 Latin American cities. *Environ. Health Perspect.* 130 (2), 1–10.
- Avila-Palencia, I., Sánchez, B.N., Rodríguez, D.A., Perez-Ferrer, C., Miranda, J.J., Gouveia, N., et al., 2022b. Health and environmental Co-benefits of city urban form in Latin America: an ecological study. *Sustain.* 14 (22), 1–14.
- Baidu Map. China Urban Vitality Research Report.
- Bakhtsiyarava, M., Schinasi, L.H., Sánchez, B.N., Dronova, I., Kephart, J.L., Ju, Y., et al., 2023. Modification of temperature-related human mortality by area-level socioeconomic and demographic characteristics in Latin American cities. *Soc. Sci. Med.* 317 (August 2022).
- Ballester, J., Quijal-Zamorano, M., Méndez Turrubiates, R.F., Pegenaute, F., Herrmann, F.R., Robine, J.M., et al., 2023. Heat-related mortality in Europe during the summer of 2022. *Nat Med* 29 (7), 1857–1866.
- Bao, Z., Bai, Y., Geng, T., 2023. Examining spatial inequalities in public green space accessibility: a focus on disadvantaged groups in England. *Sustain.* 15 (18).
- Barboza, E.P., Cirach, M., Khomenko, S., Iungman, T., Mueller, N., Barrera-Gómez, J., et al., 2021. Green space and mortality in European cities: a health impact assessment study. *Lancet Planet Heal* 5 (10), e718–e730.
- Barrington-Leigh, C., Millard-Ball, A., 2020. Global trends toward urban street-network sprawl. *Proc Natl Acad Sci U S A.* 117 (4), 1941–1950.
- Bassolas, A., Barbosa-Filho, H., Dickinson, B., Dotiwalla, X., Eastham, P., Gallotti, R., et al., 2019. Hierarchical organization of urban mobility and its connection with city livability. *Nat Commun* [Internet] 10 (1), 1–10. <https://doi.org/10.1038/s41467-019-12809-y>.
- Battiston, A., Schifanella, R., 2023. On the need to move from a single indicator to a multi-dimensional framework to measure accessibility to urban green 1–23. <http://arxiv.org/abs/2308.05538>.
- Behnisch, M., Krüger, T., Jaeger, J.A.G., 2022. Rapid rise in urban sprawl: global hotspots and trends since 1990. *PLOS Sustain Transform* 1 (11), e0000034.
- Bibri, S.E., Krogstie, J., Kärrholm, M., 2020. Compact city planning and development: emerging practices and strategies for achieving the goals of sustainability. *Dev Built Environ* 4 (June).
- Bilal, U., Hessel, P., Perez-Ferrer, C., Michael, Y.L., Alfaro, T., Tenorio-Mucha, J., et al., 2021. Life expectancy and mortality in 363 cities of Latin America. *Nat Med* 27 (3), 463–470.
- BirdLife International, 2022. World database of key biodiversity areas [Internet]. <https://www.keybiodiversityareas.org/>.
- Boeing, G., Higgs, C., Liu, S., Giles-Corti, B., Sallis, J.F., Cerin, E., et al., 2022. Using open data and open-source software to develop spatial indicators of urban design and transport features for achieving healthy and sustainable cities. *Lancet Global Health* 10 (6), e907–e918.
- Bonafoni, S., Sekertekin, A., 2020. Albedo retrieval from sentinel-2 by new narrow-to-broadband conversion coefficients. *Geosci. Rem. Sens. Lett. IEEE* 17 (9), 1618–1622.
- Brown, G., Kyttä, M., 2014. Key issues and research priorities for public participation GIS (PPGIS): a synthesis based on empirical research. *Appl. Geogr.* 46, 122–136. <https://doi.org/10.1016/j.apgeog.2013.11.004> [Internet].
- Browning, M.H.E.M., Rigolon, A., 2018. Do income, race and ethnicity, and sprawl influence the greenspace-human health link in city-level analyses? Findings from 496 cities in the United States. *Int. J. Environ. Res. Publ. Health* 15 (7).
- Burnett, R.T., Arden Pope, C., Ezzati, M., Olives, C., Lim, S.S., Mehta, S., et al., 2014. An integrated risk function for estimating the global burden of disease attributable to ambient fine particulate matter exposure. *Environ. Health Perspect.* 122 (4), 397–403.
- Carson, J.R., Conway, T.L., Perez, L.G., Frank, L.D., Saelens, B.E., Cain, K.L., et al., 2023. Neighborhood Walkability, Neighborhood Social Health, and Self-Selection Among U.S. Adults. *Heal Place* [Internet], 103036. <https://doi.org/10.1016/j.healthplace.2023.103036>, 82 (December 2022).
- Centers for Disease Control and Prevention, 2014. Behavioral Risk Factor Surveillance System 2014 (BRFSS) [Internet]. <https://www.cdc.gov/brfss/>.
- Centers for Disease Control and Prevention. 500 Cities: Local Data for Better Health. [Internet]. Available from: <https://www.cdc.gov/500cities>.
- Centers for Disease Control and Prevention. Interactive Atlas of Heart Disease and Stroke [Internet]. Available from: <https://nccd.cdc.gov/dhdsptlas/reports.aspx>.
- Centers for Disease Control and Prevention. Behavioral Risk Factor Surveillance System (BRFSS) Prevalence Data (2011 to present) [Internet]. Available from: <https://chron>

- icdata.cdc.gov/Behavioral-Risk-Factors/Behavioral-Risk-Factor-Surveillance-System-BRFSS-P/dttw-5yxu.
- Centre for International Earth Science Information Network (CIESIN), 2016. Gridded Population of the World, Version 4 (GPWv4) [Internet]. NASA Socioeconomic Data and Applications Center (SEDAC) [cited 2023 Sep 15]. <https://sedac.ciesin.columbia.edu/data/collection/gpw-v4>.
- Cerin, E., Conway, T.L., Cain, K.L., Kerr, J., De Bourdeaudhuij, I., Owen, N., et al., 2013. Sharing good NEWS across the world: developing comparable scores across 12 countries for the neighborhood environment walkability scale (NEWS). *BMC Publ. Health* 13 (1).
- Cerin, E., Sallis, J.F., Salvo, D., Hinckson, E., Conway, T.L., Owen, N., et al., 2022. Determining thresholds for spatial urban design and transport features that support walking to create healthy and sustainable cities: findings from the IPEN Adult study. *Lancet Global Health* 10 (6), e895–e906.
- Chen, J., Hoek, G., 2020. Long-term exposure to PM and all-cause and cause-specific mortality: a systematic review and meta-analysis. *Environ Int* [Internet] 143 (June), 105974. <https://doi.org/10.1016/j.envint.2020.105974>.
- Cheng, J., Xu, Z., Bambrick, H., Prescott, V., Wang, N., Zhang, Y., et al., 2019. Cardiorespiratory effects of heatwaves: a systematic review and meta-analysis of global epidemiological evidence. *Environ. Res.* 177 (April).
- China National Environmental Monitoring Centre, 2020. National air quality forecast information dissemination system. Monitoring Data [Internet]. <https://quotsoft.net/air/>.
- China economic and social big data research platform. The 6th Population Census, 2020 [Internet]. <https://data.cnki.net/%0Ayearbook/Single/N2021050059>.
- China National Urban Air Quality Real-time Publishing Platform, 2020. <https://aqicn.org/city/beijing/>.
- Chinese Statistical Yearbook, 2020. Statistical Yearbook of China [Internet]. <http://www.chinayearbooks.com/>.
- CNEMC. China National Environmental Monitoring Centre [Internet]. Available from: <https://www.cnemc.cn/en/>.
- Cohen, A.J., Brauer, M., Burnett, R., Anderson, H.R., Frostad, J., Estep, K., et al., 2017. Estimates and 25-year trends of the global burden of disease attributable to ambient air pollution: an analysis of data from the Global Burden of Diseases Study 2015. *Lancet* 389 (10082), 1907–1918. [https://doi.org/10.1016/S0140-6736\(17\)30505-6](https://doi.org/10.1016/S0140-6736(17)30505-6) [Internet].
- Cohen Hubal, E.A., Sheldon, L.S., Burke, J.M., McCurdy, T.R., Berry, M.R., Rigas, M.L., et al., 2000. Children's exposure assessment: a review of factors influencing children's exposure, and the data available to characterize and assess that exposure. *Environ. Health Perspect.* 108 (6), 475–486.
- Connolly, C., Keil, R., Ali, S.H., 2021. Extended urbanisation and the spatialities of infectious disease: demographic change, infrastructure and governance. *Urban Stud.* 58 (2), 245–263.
- Consortium, M.R.L.C., 2011. National land cover database [Internet]. <https://www.mrlc.gov/>.
- Copernicus, 2012a. Corine Land Cover 2012.
- Copernicus, 2018a. High Resolution Layers [Internet]. <https://land.copernicus.eu/pan-european/high-resolution-layers>.
- Copernicus, 2018b. Climate Variables for Cities in Europe from 2008 to 2017 [Internet]. <https://cds.climate.copernicus.eu/#1/home>.
- Copernicus.Land Monitoring Service. Tree cover density. [Internet]. Available from: <https://land.copernicus.eu/pan-european/high-resolution-layers/forests/tree-cover-density>.
- Copernicus, Urban Atlas 2012. 2012b.
- Copernicus, 2018c. Urban Atlas 2018.
- Daams, M.N., Veneri, P., 2017. Living near to attractive nature? A well-being indicator for ranking Dutch, Danish, and German functional urban areas. *Soc Indic Res* 133 (2), 501–526.
- de Hoogh, K., Chen, J., Gulliver, J., Hoffmann, B., Hertel, O., Ketzler, M., et al., 2018. Spatial PM_{2.5}, NO₂, O₃ and BC models for western Europe – evaluation of spatiotemporal stability. *Environ. Int.* 120 (2), 81–92. <https://doi.org/10.1016/j.envint.2018.07.036> [Internet].
- Deilami, K., Kamruzzaman, M., Liu, Y., 2018. Urban heat island effect: a systematic review of spatio-temporal factors, data, methods, and mitigation measures. *Int. J. Appl. Earth Obs. Geoinf.* 67 (September 2017), 30–42. <https://doi.org/10.1016/j.jag.2017.12.009> [Internet].
- Delang, M.N., Becker, J.S., Chang, K.L., Serre, M.L., Cooper, O.R., Schultz, M.G., et al., 2021. Mapping yearly fine resolution global surface ozone through the bayesian maximum entropy data fusion of observations and model output for 1990–2017. *Environ. Sci. Technol.* 55 (8), 4389–4398.
- Delcós-Alió, X., Rodríguez, D.A., Olmedo, N.L., Ferrer, C.P., Moore, K., Stern, D., et al., 2022. Is city-level travel time by car associated with individual obesity or diabetes in Latin American cities? Evidence from 178 cities in the SALURBAL project. *Cities* 131, 1–21.
- Diao, B., Ding, L., Zhang, Q., Na, J., Cheng, J., 2020. Impact of urbanization on PM_{2.5}-related health and economic loss in China 338 cities. *Int. J. Environ. Res. Publ. Health* 17 (3).
- Didan, K., 2015. MOD13Q1 MODIS/Terra Vegetation Indices 16-Day L3 Global 250m SIN Grid. NASA LP DAAC. niversity of Arizona, Alfredo Huete - University of Technology Sydney and MODAPS SIPS - NASA.
- Dijkstra, L., Florczyk, A.J., Freire, S., Kemper, T., Melchiorri, M., Pesaresi, M., et al., 2021. Applying the Degree of Urbanisation to the globe: a new harmonised definition reveals a different picture of global urbanisation. *J. Urban Econ.* 125 (November 2020), 103312 <https://doi.org/10.1016/j.jue.2020.103312> [Internet].
- Dobson, J.E., Bright, E.A., Coleman, P.R., Durfee, R.C., Worley, B.A., 2000. LandScan: a global population database for estimating populations at risk. *Photogramm Eng Remote Sensing* 66 (7), 849–857.
- Earth Engine Data Catalog, 2020a. WorldPop global project population data: estimated residential population per 100x100m grid square [Internet]. https://developers.google.com/earth-engine/datasets/catalog/WorldPop_GP_100m_pop.
- Earth Engine Data Catalog, 2020b. ESA WorldCover 10m V100 [Internet]. https://developers.google.com/earth-engine/datasets/catalog/ESA_WorldCover_v100.
- Eldesoky, A.H., Abdeldayem, W.S., 2023. Disentangling the relationship between urban form and urban resilience: a systematic literature review. *Urban Sci.* 7 (3), 93.
- Ermida, S.L., Soares, P., Mantas, V., Göttsche, F.M., Trigo, I.F., 2020. Google earth engine open-source code for land surface temperature estimation from the landsat series. *Remote Sens.* 12 (9), 1–21.
- Esch, T., Heldens, W., Hirner, A., Keil, M., Marconcini, M., Roth, A., et al., 2017. Breaking new ground in mapping human settlements from space – the Global Urban Footprint. *ISPRS J Photogramm Remote Sens* [Internet] 134, 30–42. <https://doi.org/10.1016/j.isprsjprs.2017.10.012>.
- Esperon-Rodriguez, M., Rymer, P.D., Power, S.A., Barton, D.N., Cariñanos, P., Dobbs, C., et al., 2022. Assessing climate risk to support urban forests in a changing climate. *Plants People Planet* 4 (3), 201–213.
- Essamlali, I., Nhaila, H., El Khaili, M., 2024. Supervised machine learning approaches for predicting key pollutants and for the sustainable enhancement of urban air quality: a systematic review. *Sustain. Times* 16 (3).
- European Commission, 2002. Environmental Noise Directive [Internet]. https://environment.ec.europa.eu/topics/noise/environmental-noise-directive_en.
- European Commission, 2019. City statistics [Internet]. Eurostat [cited 2023 Sep 15]. <https://ec.europa.eu/eurostat/web/main/home>.
- European Commission. Un Pacto Verde Europeo [Internet]. [cited 2023 Sep 29]. Available from: https://commission.europa.eu/strategy-and-policy/priorities-2019-2024/european-green-deal_es.
- European Commission. SHERPA [Internet]. Available from: <https://aqm.jrc.ec.europa.eu/Section/Sherpa/Document>.
- European Commissions Joint Research Centre. GHSL - Global Human Settlement Layer [Internet]. Available from: <https://ghsl.jrc.ec.europa.eu/>.
- European Environment Agency, 2006. CORINE urban morphological zones 2006 [Internet]. <https://www.eea.europa.eu/en/datahub/datahubitem-view/6e5d9b0d-a448-4c73-b008-bdd98a3cf214>.
- European Environment Agency, 2020. Environmental Noise in Europe - 2020. European Environment Agency, p. 104.
- European environment agency. Noise [Internet], 2023. <https://www.eea.europa.eu/en/topics/in-depth/noise?activeTab=fa515f0c-9ab0-493c-b4cd-58a32dfaae0a>.
- Eurostat, 2015. City Statistics. Available from: <https://ec.europa.eu/eurostat/data/data-base>.
- Eurostat. Archive: Urban-rural typology [Internet]. Available from: https://ec.europa.eu/eurostat/statistics-explained/index.php?title=Archive:Urban-rural_typology.
- Eurostat. Urban Audit [Internet]. Available from: <https://ec.europa.eu/eurostat/web/gisco/geodata/reference-data/administrative-units-statistical-units/urban-audit>.
- Eurostat. What is a city? - Spatial units [Internet]. Available from: <https://ec.europa.eu/eurostat/web/cities/spatial-units>.
- Fagliano, J.A., Roux, A.V.D., 2018. Climate change, urban health, and the promotion of health equity. *PLoS Med.* 8–11.
- Fazeli Dehkordi, Z.S., Khatami, S.M., Ranjbar, E., 2022. The associations between urban form and major non-communicable diseases: a systematic review. *J. Urban Health* 99, 941–958.
- Geng, G., Xiao, Q., Liu, S., Liu, X., Cheng, J., Zheng, Y., et al., 2021. Tracking air pollution in China: near real-time PM_{2.5} retrievals from multisource data fusion. *Environ. Sci. Technol.* 55 (17), 12106–12115.
- Giles-Corti, B., Vernez-Moudon, A., Reis, R., Turrell, G., Dannenberg, A.L., Badland, H., et al., 2016. City planning and population health: a global challenge. *Lancet* 388 (10062), 2912–2924. [https://doi.org/10.1016/S0140-6736\(16\)30066-6](https://doi.org/10.1016/S0140-6736(16)30066-6) [Internet].
- Giles-Corti, B., Moudon, A.V., Lowe, M., Cerin, E., Boeing, G., Frumkin, H., et al., 2022. What next? Expanding our view of city planning and global health, and implementing and monitoring evidence-informed policy. *Lancet Global Health* 10 (6), e919–e926.
- Glazener, A., Sanchez, K., Ramani, T., Zietsman, J., Nieuwenhuijsen, M.J., Mindell, J.S., et al., 2021a. Fourteen pathways between urban transportation and health: a conceptual model and literature review. *J Transp Heal* [Internet] 21 (February), 101070. <https://doi.org/10.1016/j.jth.2021.101070>.
- Glazener, A., Sanchez, K., Ramani, T., Zietsman, J., Nieuwenhuijsen, M.J., Mindell, J.S., et al., 2021b. Fourteen pathways between urban transportation and health: a conceptual model and literature review. *J Transp Heal* [Internet] 21 (April), 101070. <https://doi.org/10.1016/j.jth.2021.101070>.
- Global Biodiversity Information Faculty, 2022. Occurrence download-birds [internet]. <https://www.gbif.org/occurrence/download/0197178-210914110416597>.
- Google. Location history [Internet]. Available from: <https://support.google.com/accounts/answer/3118687>.
- Gouveia, N., Kephart, J.L., Dronova, I., McClure, L., Granados, J.T., Betancourt, R.M., et al., 2021. Ambient fine particulate matter in Latin American cities: levels, population exposure, and associated urban factors. *Sci Total Environ* [Internet] 772, 145035. <https://doi.org/10.1016/j.scitotenv.2021.145035>.
- Granier, C., Darras, S., Denier van der Gon H, Doubalova, J., Elguindi, N., Galle, B., et al., 2019. The Copernicus Atmosphere monitoring service global and regional emissions. *Copernicus Atmos Monit Serv*, p. 54 (April).
- Guan, Y., Kang, L., Wang, Y., Zhang, N.N., Ju, M.T., 2019. Health loss attributed to PM_{2.5} pollution in China's cities: economic impact, annual change and reduction potential. *J. Clean. Prod.* 217, 284–294.

- Guan, Y., Xiao, Y., Wang, F., Qiu, X., Zhang, N., 2021a. Health impacts attributable to ambient PM_{2.5} and ozone pollution in major Chinese cities at seasonal-level. *J. Clean. Prod.* 311 (January).
- Guan, Y., Xiao, Y., Wang, Y., Zhang, N., Chu, C., 2021b. Assessing the health impacts attributable to PM_{2.5} and ozone pollution in 338 Chinese cities from 2015 to 2020. *Environ Pollut* 287 (February), 117623. <https://doi.org/10.1016/j.envpol.2021.117623> [Internet].
- Guan, Y., Xiao, Y., Zhang, N., Chu, C., 2022a. Tracking short-term health impacts attributed to ambient PM_{2.5} and ozone pollution in Chinese cities: an assessment integrates daily population. *Environ Sci Pollut Res* [Internet] 29 (60), 91176–91189. <https://doi.org/10.1007/s11356-022-22067-z>.
- Guan, Y., Xiao, Y., Chu, C., Zhang, N., Yu, L., 2022b. Trends and characteristics of ozone and nitrogen dioxide related health impacts in Chinese cities. *Ecotoxicol. Environ. Saf.* 241 (June).
- Guski, R., Schreckenber, D., Schuemer, R., 2017. WHO environmental noise guidelines for the European region: a systematic review on environmental noise and annoyance. *Int. J. Environ. Res. Publ. Health* 14 (12), 1–39.
- Guthold, R., Stevens, G.A., Riley, L.M., Bull, F.C., 2018. Worldwide trends in insufficient physical activity from 2001 to 2016: a pooled analysis of 358 population-based surveys with 1·9 million participants. *Lancet Glob Heal* [Internet] 6 (10), e1077–e1086. [https://doi.org/10.1016/S2214-109X\(18\)30357-7](https://doi.org/10.1016/S2214-109X(18)30357-7).
- Hammer, M.S., Van Donkelaar, A., Li, C., Lyapustin, A., Sayer, A.M., Hsu, N.C., et al., 2020. Global estimates and long-term trends of fine particulate matter concentrations (1998–2018). *Environ. Sci. Technol.* 54 (13), 7879–7890.
- Han, C., Xu, R., Ye, T., Xie, Y., Zhao, Y., Liu, H., et al., 2022. Mortality burden due to long-term exposure to ambient PM_{2.5} above the new WHO air quality guideline based on 296 cities in China. *Environ Int* [Internet] 166 (May), 107331. <https://doi.org/10.1016/j.envint.2022.107331>.
- Harris, N.L., Gibbs, D.A., Baccini, A., Birdsey, R.A., de Bruin, S., Farina, M., et al., 2021. Global maps of twenty-first century forest carbon fluxes. *Nat Clim Chang* [Internet] 11 (3), 234–240. <https://doi.org/10.1038/s41558-020-00976-6>.
- Henson, J., De Craemer, M., Yates, T., 2023. Sedentary behaviour and disease risk. *BMC Publ. Health* 23 (1), 23–25.
- Hersbach, H., Bell, B., Berrisford, P., Hirahara, S., Horányi, A., Muñoz-Sabater, J., et al., 2020. The ERA5 global reanalysis. *Q. J. R. Meteorol. Soc.* 146 (730), 1999–2049.
- Heydari, S., Asgharian, M., Kelly, F.J., Goel, R., 2022. Potential health benefits of eliminating traffic emissions in urban areas. *PLoS One* [Internet] 17 (3 March), 1–14. <https://doi.org/10.1371/journal.pone.0264803>.
- Hoffmann, E., Barros, H., Ribeiro, A.I., 2017. Socioeconomic inequalities in green space quality and Accessibility—evidence from a Southern European city. *Int. J. Environ. Res. Publ. Health* 14 (8).
- Huangfu, P., Atkinson, R., 2020. Long-term exposure to NO₂ and O₃ and all-cause and respiratory mortality: a systematic review and meta-analysis. *Environ. Int.* 144 (July), 105998 <https://doi.org/10.1016/j.envint.2020.105998> [Internet].
- Inness, A., Aedes, M., Agustí-Panareda, A., Barré, J., Benedictow Alebschmidt, A., Dominguez, J., et al., 2019. CAMS global reanalysis (EAC4). Copernicus Atmosphere Monitoring Service [Internet]. <https://ads.atmosphere.copernicus.eu/cdsapp%23/dataset/cams-global-reanalysis-eac4?tab=overview>.
- Institute for Health Metrics and Evaluation. Global Burden of Disease (GBD) [Internet]. Available from: <https://www.healthdata.org/research-analysis/gbd>.
- Institute for Health Metrics and Evaluation GHDX, 2010. Global burden of disease study 2010 (GBD 2010) - ambient air pollution risk model 1990 - 2010 [Internet]. <http://ghdx.healthdata.org/record/ihme-data/gbd-2010-ambient-air-pollution-risk-model-1990-2010>.
- Institute for Health Metrics and Evaluation's Global Burden of Disease, Institute HE, 2020. State of global air report 2020 [Internet]. <https://www.stateofglobalair.org/research-report/state-global-air-report-2020>.
- Iungman, T., Cirach, M., Marando, F., Pereira Barboza, E., Khomenko, S., Masselot, P., et al., 2023. Cooling cities through urban green infrastructure: a health impact assessment of European cities. *Lancet* 401 (10376), 577–589.
- Jerrett, M., Burnett, R.T., Pope, C.A., Ito, K., Thurston, G., Krewski, D., et al., 2009. Long-term ozone exposure and mortality. *N. Engl. J. Med.* 360 (11), 1085–1095.
- Jia, P., Chen, C., Zhang, D., Sang, Y., Zhang, L., 2024. Semantic segmentation of deep learning remote sensing images based on band combination principle: application in urban planning and land use. *Comput. Commun.* 217 (November 2023), 97–106.
- Joffe, M., Mindell, J., 2005. Health impact assessment. *Occup. Environ. Med.* 62 (12), 907–912.
- Kan, H.D., Chen, B.H., 2002. Analysis of exposure response relationships of air particulate matter and adverse health outcomes in China. *J. Environ. Health* 19, 422–424.
- Kephart, J.L., Sánchez, B.N., Moore, J., Schinasi, L.H., Bakhtsiyarava, M., Ju, Y., et al., 2022. City-level impact of extreme temperatures and mortality in Latin America. *Nat Med* 28 (8), 1700–1705.
- Kephart, J.L., Gouveia, N., Rodriguez, D.A., Indvik, K., Alfaro, T., Texcalac, J.L., Miranda Jj Bu, Ra, 2023. Ambient nitrogen dioxide in 47,187 neighborhoods across 1 326 cities in eight Latin 2 American countries: population exposures and associations with urban features. *medRxiv* 1–21.
- Khomenko, S., Cirach, M., Pereira-Barboza, E., Mueller, N., Barrera-Gómez, J., Rojas-Rueda, D., et al., 2021. Premature mortality due to air pollution in European cities: a health impact assessment. *Lancet Planet Heal* 5 (3), e121–e134.
- Khomenko, S., Cirach, M., Barrera-Gómez, J., Pereira-Barboza, E., Iungman, T., Mueller, N., et al., 2022. Impact of road traffic noise on annoyance and preventable mortality in European cities: a health impact assessment. *Environ. Int.* 162 (December 2021).
- Khomenko, S., Pisoni, E., Thunis, P., Bessagnet, B., Cirach, M., Iungman, T., et al., 2023. Spatial and sector-specific contributions of emissions to ambient air pollution and mortality in European cities: a health impact assessment. *Lancet Public Heal* [Internet] 8 (7), e546–e558. [https://doi.org/10.1016/S2468-2667\(23\)00106-8](https://doi.org/10.1016/S2468-2667(23)00106-8).
- Kirmse, A., Udeshi, T., Bellver, P., Shuma, J., 2011. Extracting patterns from location history. *GIS Proc ACM Int Symp Adv Geogr Inf Syst.* 397–400.
- Klimont, Z., Kupiainen, K., Heyes, C., Purohit, P., Cofala, J., Rafaj, P., et al., 2017. Global anthropogenic emissions of particulate matter including black carbon. *Atmos. Chem. Phys.* 17 (14), 8681–8723.
- Köppen-Geiger climate classification system. Köppen-Geiger climate classification maps and bioclimatic variables [Internet]. Available from: <http://glass.umd.edu/KGClim/>.
- Krummenauer, L., Prah, B.F., Costa, L., Holsten, A., Walther, C., Kropp, J.P., 2019. Global drivers of minimum mortality temperatures in cities. *Sci. Total Environ.* 695, 133560 <https://doi.org/10.1016/j.scitotenv.2019.07.366> [Internet].
- Kuenen, J., Dellaert, S., Visschedijk, A., Jalkanen, J.P., Super, I., Denier Van Der Gon, H., 2022. CAMS-REG-v4: a state-of-the-art high-resolution European emission inventory for air quality modelling. *Earth Syst. Sci. Data* 14 (2), 491–515.
- Kummu, M., Taka, M., Guillaume, J.H.A., 2018. Gridded global datasets for gross domestic product and human development index over 1990–2015. *Sci. Data* 5, 1–15.
- Larkin, A., Geddes, J.A., Martin, R.V., Xiao, Q., Liu, Y., Marshall J D Brauer M Hystad P, 2017. A global land use regression model for nitrogen dioxide air pollution. *Physiol Behav* [Internet] 176 (5), 139–148. <https://www.ncbi.nlm.nih.gov/pmc/articles/PMC5958625/pdf/nihms960157.pdf>.
- Lenzi, A., 2019. Why urbanisation and health? *Acta Biomed.* 90 (2), 181–183.
- Liu, N., Liu, W., Deng, F., Liu, Y., Gao, X., Fang, L., et al., 2023. The burden of disease attributable to indoor air pollutants in China from 2000 to 2017. *Lancet Planet Heal.* 7 (11), e900–e911.
- Washington University in St. Louis. Atmospheric Composition Analysis Group [Internet]. Available from: <https://sites.wustl.edu/acag/>.
- Lowe, M., Adlakha, D., Sallis, J.F., Salvo, D., Cerin, E., Moudon, A.V., et al., 2022. City planning policies to support health and sustainability: an international comparison of policy indicators for 25 cities. *Lancet Global Health* 10 (6), e882–e894.
- Luxen, D., Vetter, C., 2011. Real-time routing with OpenStreetMap data. *GIS Proc ACM Int Symp Adv Geogr Inf Syst*, pp. 513–516.
- Mackres, E., Shabou, S., Wong, T., 2023. Calculating Indicators from Global Geospatial Data Sets for Benchmarking and Tracking Change in the Urban Environment. *World Resour Inst*, pp. 1–36 (March).
- Maji, K.J., Arora, M., Dikshit, A.K., 2017. Burden of disease attributed to ambient PM_{2.5} and PM₁₀ exposure in 190 cities in China. *Environ. Sci. Pollut. Res.* 24 (12), 11559–11572.
- Maji, K.J., Ye, W.F., Arora, M., Shiva Nagendra, S.M., 2018. PM_{2.5}-related health and economic loss assessment for 338 Chinese cities. *Environ. Int.* 121 (April), 392–403. <https://doi.org/10.1016/j.envint.2018.09.024> [Internet].
- Maji, K.J., Ye, W.F., Arora, M., Nagendra, S.M.S., 2019. Ozone pollution in Chinese cities: assessment of seasonal variation, health effects and economic burden. *Environ Pollut* [Internet] 247 (x), 792–801. <https://doi.org/10.1016/j.envpol.2019.01.049>.
- Malashock, D.A., Delang, M.N., Becker, J.S., Serre, M.L., West, J.J., Chang, K.L., et al., 2022a. Global trends in ozone concentration and attributable mortality for urban, peri-urban, and rural areas between 2000 and 2019: a modelling study. *Lancet Planet Heal* [Internet] 6 (12), e958–e967. [https://doi.org/10.1016/S2542-5196\(22\)00260-1](https://doi.org/10.1016/S2542-5196(22)00260-1).
- Malashock, D.A., Delang, M.N., Becker, J.S., Serre, M.L., West, J.J., Chang, K.L., et al., 2022b. Estimates of ozone concentrations and attributable mortality in urban, peri-urban and rural areas worldwide in 2019. *Environ. Res. Lett.* 17 (5).
- Marando, F., Heris, M.P., Zulfan, G., Udiás, A., Mentaschi, L., Chrysoulakis, N., et al., 2022. Urban heat island mitigation by green infrastructure in European Functional Urban Areas. *Sustain Cities Soc* [Internet] 77 (November 2021), 103564. <https://doi.org/10.1016/j.scs.2021.103564>.
- Masselot, P., Mistry, M., Vanoli, J., Schneider, R., Iungman, T., Garcia-Leon, D., et al., 2023. Excess mortality attributed to heat and cold: a health impact assessment study in 854 cities in Europe. *Lancet Planet Heal* 7 (4), e271–e281.
- McDonald, R.I., Aronson, M.F.J., Beatley, T., Beller, E., Bazo, M., Grossinger, R., et al., 2023. Denser and greener cities: green interventions to achieve both urban density and nature. *People Nat* 5 (1), 84–102.
- Mead, R.W., Brajer, V., 2006. Valuing the adult health effects of air pollution in Chinese cities. *Ann. N. Y. Acad. Sci.* 1076, 882–892.
- Mejía-Dorantes, L., Soto Villagrán, P., 2020. A review on the influence of barriers on gender equality to access the city: a synthesis approach of Mexico City and its Metropolitan Area. *Cities* 96 (October).
- Meng, X., Liu, C., Chen, R., Sera, F., Vicedo-Cabrera, A.M., Milojevic, A., et al., 2021. Short term associations of ambient nitrogen dioxide with daily total, cardiovascular, and respiratory mortality: multilocation analysis in 398 cities. *BMJ* 372 (2).
- Ministry of Environmental Protection. Technical Regulation for Ambient Air Quality Assessment. Available from: https://www.gov.il/en/departments/ministry_of_environmental_protection/govil-landing-page.
- Mir, M., Nasirzadeh, F., Bereznicki, H., Enticott, P., Lee, S.H., Mills, A., 2023. Construction noise effects on human health: evidence from physiological measures. *Sustain Cities Soc* [Internet] 91 (November 2022), 104470. <https://doi.org/10.1016/j.scs.2023.104470>.
- Moran, D., Kanemoto, K., Jiborn, M., Wood, R., Többen, J., Seto, K.C., 2018. Carbon footprints of 13 000 cities. *Environ. Res. Lett.* 13 (6).
- Moriconi-Ebrardi, Francis, Harre, Dominic, Heinriqs, P., 2016. Urbanisation Dynamics in West Africa 1950–2010: Africapolis I. OECD Publishing, Paris.
- Motieyan, H., Mesgari, M.S., 2018. An Agent-Based Modeling approach for sustainable urban planning from land use and public transit perspectives. *Cities* [Internet] 81 (March), 91–100. <https://doi.org/10.1016/j.cities.2018.03.018>.
- Mueller, N., Rojas-Rueda, D., Khreis, H., Cirach, M., Milà, C., Espinosa, A., et al., 2018. Socioeconomic inequalities in urban and transport planning related exposures and

- mortality: a health impact assessment study for Bradford, UK. *Environ. Int.* 121, 931–941.
- Mueller, N., Anderle, R., Brachowicz, N., Graziadei, H., Lloyd, S.J., Morais, D.S., et al., 2023. Model choice for quantitative health impact assessment and modelling: an expert consultation and narrative literature review. *Kerman Univ Med Sci* [Internet] 12, 7103. <https://doi.org/10.34172/ijhpm.2023.7103>.
- Mullachery, P.H., Rodriguez, D.A., Miranda, J.J., López-Olmedo, N., Martínez-Folgar, K., Barreto, M.L., et al., 2022. Mortality amenable to healthcare in Latin American cities: a cross-sectional study examining between-country variation in amenable mortality and the role of urban metrics. *Int. J. Epidemiol.* 51 (1), 303–313.
- Muñoz-Sabater, J., Dutra, E., Agustí-Panareda, A., Albergel, C., Arduini, G., Balsamo, G., et al., 2021. ERA5-Land: a state-of-the-art global reanalysis dataset for land applications. *Earth Syst. Sci. Data* 13 (9), 4349–4383.
- Naghavi, M., Abajobir, A.A., Abbafati, C., Abbas, K.M., Abd-Allah, F., Abera, S.F., et al., 2017. Global, regional, and national age-sex specific mortality for 264 causes of death, 1980–2016: a systematic analysis for the Global Burden of Disease Study 2016. *Lancet.* 390 (10100), 1151–1210.
- National Bureau of Statistical of China, 2016. China Statistical Yearbook 2014 [Internet]. <http://www.stats.gov.cn/tjsj/ndsj/%0A2014/indexeh.htm>.
- National Bureau of Statistics of China, 2021. Main Data of the Seventh National Population Census [Internet]. http://www.stats.gov.cn/english/PressRelease/202105/t20210510_1817185.html.
- Nguyen, Q.C., Khanna, S., Dwivedi, P., Huang, D., Huang, Y., Tasdizen, T., et al., 2019. Using Google Street View to examine associations between built environment characteristics and U.S. health outcomes. *Prev Med Reports* 14 (April), 100859. <https://doi.org/10.1016/j.pmedr.2019.100859> [Internet].
- Nieuwenhuijsen, M.J., 2016. Urban and transport planning, environmental exposures and health-new concepts, methods and tools to improve health in cities. *Environ Heal A Glob Access Sci Source* 15 (Suppl. 1).
- Nieuwenhuijsen, M.J., 2020. Urban and transport planning pathways to carbon neutral, liveable and healthy cities: A review of the current evidence. *Environ Int* [Internet] 140, 105661. <https://doi.org/10.1016/j.envint.2020.105661>. April.
- Nieuwenhuijsen, M.J., Khreis, H., 2016. Car free cities: pathway to healthy urban living. *Environ. Int.* 94, 251–262. <https://doi.org/10.1016/j.envint.2016.05.032> [Internet].
- Nieuwenhuijsen, M., de Nazelle, A., Pradas, M.C., Daher, C., Dzhambov, A.M., Echave, C., et al., 2024. The Superblock model: a review of an innovative urban model for sustainability, liveability, health and well-being. *Environ. Res.* 251 (March).
- NOAA National Climatic Data Center, 2018. Global Summary of the Day (GSOD).
- Oda, T., Maksyutov, S., 2011. A very high-resolution (1 km×1 km) global fossil fuel CO₂ emission inventory derived using a point source database and satellite observations of nighttime lights. *Atmos. Chem. Phys.* 11, 543–556.
- OECD/SWAC. Africapolis database Internet, 2018. OECD and Sahel and West Africa Club. OECD Publishing, Paris. <https://africapolis.org>.
- Oh, J.W., Ngarambe, J., Duhirwe, P.N., Yun, G.Y., Santamouris, M., 2020. Using deep-learning to forecast the magnitude and characteristics of urban heat island in Seoul Korea. *Sci Rep* [Internet] 10 (1), 1–13. <https://doi.org/10.1038/s41598-020-60632-z>.
- Oke, C., Bekesy, S.A., Frantzeskaki, N., Bush, J., Fitzsimons, J.A., Garrard, G.E., et al., 2021. Cities should respond to the biodiversity extinction crisis. *npj Urban Sustain* [Internet] 1 (1), 9–12. <https://doi.org/10.1038/s42949-020-00010-w>.
- Olsen, J.R., Nicholls, N., Moon, G., Pearce, J., Shortt, N., Mitchell, R., 2019. Which urban land covers/uses are associated with residents' mortality? A cross-sectional, ecological, pan-European study of 233 cities. *BMJ Open* 9 (11).
- Open Street Map, 2017. OpenStreetMap Contributors [Internet]. <https://www.openstreetmap.org>.
- OpenStreetMap [Internet], 2022. <https://www.openstreetmap.org/#map=6/40.011/-2.483>.
- Orellano, P., Reynoso, J., Quaranta, N., Bardach, A., Ciapponi, A., 2020. Short-term exposure to particulate matter (PM₁₀ and PM_{2.5}), nitrogen dioxide (NO₂), and ozone (O₃) and all-cause and cause-specific mortality: systematic review and meta-analysis. *Environ Int* [Internet] 142 (December 2019), 105876. <https://doi.org/10.1016/j.envint.2020.105876>.
- Ortigoza, A.F., Tapia Granados, J.A., Miranda, J.J., Alazraqui, M., Higuera, D., Villamonte, G., et al., 2021. Characterising variability and predictors of infant mortality in urban settings: findings from 286 Latin American cities. *J. Epidemiol. Community Health* 75 (3), 264–270.
- Parastatidis, D., Mittra, Z., Chrysoulakis, N., Abrams, M., 2017. Online global land surface temperature estimation from landsat. *Remote Sens* 9 (12), 1–16.
- Park, J.H., Moon, J.H., Kim, H.J., Kong, M.H., Oh, Y.H., 2020. Sedentary lifestyle: overview of updated evidence of potential health risks. *Korean J Fam Med.* 41 (6), 365–373.
- Pesaresi, M., Florczyk, A., Schiavina, M., Melchiorri, M.M.L., 2019. GHS-SMOD R2019A - GHS settlement layers, updated and refined REGIO model 2014. In: Application to GHS-BUILT R2018A and GHS-POP R2019A, Multitemporal (1975-1990-2000-2015) [Internet]. <https://data.jrc.ec.europa.eu/dataset/42e8be89-54ff-464e-be7b-bf9e64da5218>.
- Peters, M.D.J., Marnie, C., Colquhoun, H., Garrity, C.M., Hempel, S., Horsley, T., et al., 2021. Scoping reviews: reinforcing and advancing the methodology and application. *Syst. Rev.* 10 (1), 1–6.
- Phillips, A., Canters, F., Khan, A.Z., 2022. Analyzing spatial inequalities in use and experience of urban green spaces. *Urban For Urban Green* [Internet] 74 (January), 127674. <https://doi.org/10.1016/j.ufug.2022.127674>.
- Pisoni, E., Thunis, P., Clappier, A., 2019. Application of the SHERPA source-receptor relationships, based on the EMEP MSC-W model, for the assessment of air quality policy scenarios. *Atmos. Environ.* X 4 (April), 100047. <https://doi.org/10.1016/j.aeoa.2019.100047> [Internet].
- Prieto-Curiel, R., Heinrichs, P., Heo, I., 2017. Cities and Spatial Interactions in West Africa: A Clustering Analysis of the Local Interactions of Urban Agglomerations. *OECD Publ.*, 05.
- Prieto-Curiel, R., Patino, J.E., Anderson, B., 2023. Scaling of the morphology of African cities. *Proc Natl Acad Sci U S A.* 120 (9), 1–9.
- Puttaswamy, D., Ghosh, S., Kuriyan, R., 2023. Neighborhood walkability index and its association with indices of childhood obesity in Bengaluru, Karnataka. *Indian Pediatr.* 60 (2), 113–118.
- Quistberg, D.A., Roux, A.V.D., Bilal, U., Moore, K., Ortigoza, A., Rodriguez, D.A., et al., 2019. Building a Data Platform for Cross-Country Urban Health Studies: the SALURBAL Study, pp. 311–337.
- Resource Watch. Trees in Mosaic Landscapes [Internet]. Available from: <https://resource-watch.org/data/explore/Trees-in-Mosaic-Landscapes>.
- Rezaei, N., Millard-Ball, A., 2023. Urban form and its impacts on air pollution and access to green space: a global analysis of 462 cities. *PLoS One* [Internet] 18 (1 January), 1–26. <https://doi.org/10.1371/journal.pone.0278265>.
- Richardson, E.A., Moon, G., Pearce, J., Shortt, N.K.M.R., 2017. Multi-scalar influences on mortality change over time in 274 European cities. *Soc. Sci. Med.* 179, 45–51. [Internet] <https://pubmed.ncbi.nlm.nih.gov/28254658/>.
- Ritchie, H., 2023. Global inequalities in CO₂ emissions. [Internet]. *OurWorldInData.org*. <https://ourworldindata.org/inequality-co2>.
- Romero-Lankao, P., Qin, H., Dickinson, K., 2012. Urban vulnerability to temperature-related hazards: a meta-analysis and meta-knowledge approach. *Glob Environ Chang* 22 (3), 670–683. <https://doi.org/10.1016/j.gloenvcha.2012.04.002> [Internet].
- Rybski, D., Arcaute, E., Batty, M., 2019. Urban scaling laws. *Environ. Plan. B Urban Anal. City Sci.* 46 (9), 1605–1610.
- Sarkar, C., Webster, C., 2017. Healthy cities of tomorrow: the case for large scale built environment-health studies. *J Urban Heal* 94 (1), 4–19.
- Sarmiento, O.L., Useche, A.F., Rodriguez, D.A., Dronova, I., Guaje, O., Montes, F., et al., 2021. Built environment profiles for Latin American urban settings: the SALURBAL study. *PLoS One* 16 (10 October), 1–25.
- Schiavina, M., Moon, G., Pearce, J., Shortt, N.K.M.R., 2019. GHS-POP R2019A - GHS Population Grid Multitemporal (1975-1990-2000-2015) - OBSOLETE RELEASE. European Commission [Internet].
- Shaddick, G., Thomas, M.L., Amini, H., Broday, D., Cohen, A., Frostad, J., et al., 2018. Data integration for the assessment of population exposure to ambient air pollution for global burden of disease assessment. *Environ. Sci. Technol.* 52 (16), 9069–9078.
- Shashank, A., Schuurman, N., 2019. Unpacking Walkability Indices and Their Inherent Assumptions. *Heal Place* [Internet], pp. 145–154. <https://doi.org/10.1016/j.healthplace.2018.12.005>, 55(June 2018).
- Simpson, D., Benedictow, A., Berge, H., Bergström, R., Emberson, L.D., Fagerli, H., et al., 2012. The EMEP MSC-W chemical transport model – technical description. *Atmos. Chem. Phys.* 12 (16), 7825–65.
- Smith, N., Georgiou, M., King, A.C., Tiegies, Z., Webb, S., Chastin, S., 2021. Urban blue spaces and human health: a systematic review and meta-analysis of quantitative studies. *Cities* 119 (May).
- Solomon, D.S., Singh, C., Islam, F., 2021. Examining the outcomes of urban adaptation interventions on gender equality using SDG 5. *Clim Dev* [Internet] 13 (9), 830–841. <https://doi.org/10.1080/17565529.2021.1939643>.
- Son, T.H., Weedon, Z., Yigitcanlar, T., Sanchez, T., Corchado, J.M., Mehmood, R., 2023. Algorithmic urban planning for smart and sustainable development: systematic review of the literature. *Sustain Cities Soc* [Internet] 94 (March), 104562. <https://doi.org/10.1016/j.scs.2023.104562>.
- Song, J., Wang, Y., Zhang, Q., Qin, W., Pan, R., Yi, W., et al., 2023. Premature mortality attributable to NO₂ exposure in cities and the role of built environment: a global analysis. *Sci. Total Environ.* 866 (2), 161395 <https://doi.org/10.1016/j.scitotenv.2023.161395> [Internet].
- Southerland, V.A., Brauer, M., Mohegh, A., Hammer, M.S., van Donkelaar, A., Martin, R.V., et al., 2022. Global urban temporal trends in fine particulate matter (PM_{2.5}) and attributable health burdens: estimates from global datasets. *Lancet Planet Heal* [Internet] 6 (2), e139–e146. [https://doi.org/10.1016/S2542-5196\(21\)00350-8](https://doi.org/10.1016/S2542-5196(21)00350-8).
- Stafoggia, M., Tobias, A., Chen, H., Burnett, R.T., 2022. Differential mortality risks associated with PM_{2.5} components: a multi-country, multi-city study. *Epidemiology* 33 (2), 167–175.
- Stanaway, J.D., Afshin, A., Gakidou, E., Lim, S.S., Abate, D., Abate, K.H., et al., 2017. Global, regional, and national comparative risk assessment of 84 behavioural, environmental and occupational, and metabolic risks or clusters of risks for 195 countries and territories, 1990–2017: a systematic analysis for the Global Burden of Disease Stu. *Lancet* 392 (10159), 1923–1994.
- State Environmental Protection Administration of China (SEPA), 2005. Annual Report of National Urban Environmental Management and Integrated Management in 2004.
- Stieb, D.M., Berjawi, R., Emode, M., Zheng, C., Salama, D., Hocking, R., et al., 2021. Systematic review and meta-analysis of cohort studies of long term outdoor nitrogen dioxide exposure and mortality. *PLoS One* [Internet] 16 (2 February), 1–20. <https://doi.org/10.1371/journal.pone.0246451>.
- Stockton, J.C., Duke-Williams, O., Stamatakis, E., Mindell, J.S., Brunner, E.J., Shelton, N.J., 2016. Development of a novel walkability index for London, United Kingdom: cross-sectional application to the Whitehall II Study. *BMC Publ. Health* 16 (1), 1–12. <https://doi.org/10.1186/s12889-016-3012-2> [Internet].
- Stohl, A., Aamaas, B., Amann, M., Baker, L.H., Bellouin, N., Bernsten, T.K., et al., 2015. Evaluating the climate and air quality impacts of short-lived pollutants. *Atmos. Chem. Phys.* 15 (18), 10529–10566.
- Stowell, J.D., Ngo, C., Jimenez, M.P., Kinney, P.L., James, P., 2023. Development of a global urban greenness indicator dataset for 1,000+ cities. *Data Br* 48, 109140. <https://doi.org/10.1016/j.dib.2023.109140> [Internet].

- TAP Internet. Available from: <http://tapdata.org.cn>.
- Taubenböck, H., Debray, H., Qiu, C., Schmitt, M., Wang, Y., Zhu, X.X., 2020. Seven city types representing morphologic configurations of cities across the globe. *Cities* 105 (April), 102814. <https://doi.org/10.1016/j.cities.2020.102814> [Internet].
- The Lancet, 2022. Urban design, transport and health [Internet] [cited 2023 Sep 28]. <https://www.thelancet.com/series/urban-design-2022>.
- The Urban Burden of Disease Estimation for Policy Making. UBDPolicy: Assessing the burden of disease of urban life in 1000 European cities [Internet]. Available from: <https://ubdpolicy.eu/>.
- The World Bank. Urban Development [Internet]. [cited 2023 Sep 20]. Available from: <https://www.worldbank.org/en/topic/urbandevelopment/overview>.
- The World Bank, 2016. The World Bank Open Data [Internet]. <https://data.worldbank.org/>.
- The Multi-Country Multi-City (MCC) Collaborative Research Network. London School of Hygiene & Tropical Medicine. Available from: <https://mccstudy.lshtm.ac.uk/>.
- The World Bank United Nations Population Division. World Urbanization Prospects: 2018 Revision. [Internet]. [cited 2023 Sep 20]. Available from: <https://data.worldbank.org/indicator/SP.URB.TOTL.IN.ZS>.
- Thompson, R., Hornigold, R., Page, L., Waite, T., 2018. Associations between high ambient temperatures and heat waves with mental health outcomes: a systematic review. *Publ. Health* 161, 171–191. <https://doi.org/10.1016/j.puhe.2018.06.008> [Internet].
- Thompson, J., Stevenson, M., Wijnands, J.S., Nice, K.A., Aschwanden, G.D., Silver, J., et al., 2020. A global analysis of urban design types and road transport injury: an image processing study. *Lancet Planet Heal* 4 (1), e32–e42.
- Thondoo, M., Rojas-Rueda, D., Gupta, J., De Vries, D.H., Nieuwenhuijsen, M.J., 2019. Systematic literature review of health impact assessments in low and middle-income countries. *Int. J. Environ. Res. Publ. Health* 16 (11).
- Thrasher, B., Maurer, E.P., McKellar, C., Duffy, P.B., 2012. Technical Note: bias correcting climate model simulated daily temperature extremes with quantile mapping. *Hydrol. Earth Syst. Sci.* 16 (9), 3309–3314.
- Tonne, C., Adair, L., Adlakha, D., Anguelovski, I., Belesova, K., Berger, M., et al., 2021. Defining pathways to healthy sustainable urban development. *Environ. Int.* 146.
- Turner, M.C., Jerrett, M., Pope, C.A., Krewski, D., Gapstur, S.M., Diver, W.R., et al., 2016. Long-term ozone exposure and mortality in a large prospective study. *Am. J. Respir. Crit. Care Med.* 193 (10), 1134–1142.
- UN General Assembly, 2015. Resolution adopted by the General Assembly: transforming our world: the 2030 agenda for sustainable development. Transform our world 2030 Agenda Sustain Dev [Internet] 259–273, 16301(October). https://www.un.org/en/development/desa/population/migration/generalassembly/docs/globalcompact/A_RES_70_1_E.pdf.
- UNECE, 2017. Smart Sustainable Cities [Internet] [cited 2023 Sep 28]. <https://unece.org/housing/smart-sustainable-cities>.
- United Nations. The Paris Agreement [Internet]. [cited 2023 Sep 29]. Available from: <https://unfccc.int/process-and-meetings/the-paris-agreement>.
- United Nations Department of Economic and Social Affairs Population Department, 2014. World Urbanization Prospects: the 2014 Revision, CD-ROM edition. Data publication [Internet]. <https://population.un.org/wup/>.
- United Nations Development Program, 2022. Human Development Report [Internet] [cited 2023 Sep 28]. <https://hdr.undp.org/>.
- United Nations Development Programme, 2008. Millennium Development Goals. Lebanon Report, vol. 2.
- United States Census Bureau. Longitudinal Employer-Household Dynamics [Internet]. Available from: <https://lehd.ces.census.gov/data/>.
- United States Census Bureau, 2016. TIGER/Line shapefiles. <https://www.census.gov/geographies/mapping-files/time-series/geo/tiger-line-file.html>.
- United States Geological Survey. Landsat [Internet]. Available from: <https://earthexplorer.usgs.gov/>.
- University D. Urban Health Collaborative [Internet]. Available from: <https://drexel.edu/uhc/>.
- U.S. Department of Transportation. Transportation health tool indicators [Internet]. Available from: <https://www.transportation.gov/>.
- van Kempen, E., Casas, M., Pershagen, G., Foraster, M., 2018. WHO environmental noise guidelines for the European region: a systematic review on environmental noise and cardiovascular and metabolic effects: a summary. *Int. J. Environ. Res. Publ. Health* 15 (2), 1–59.
- Van Tran, V., Park, D., Lee, Y.C., 2020. Indoor air pollution, related human diseases, and recent trends in the control and improvement of indoor air quality. *Int. J. Environ. Res. Publ. Health* 17 (8).
- Wang, Y., Shi, L., Zanobetti, A., Schwartz, J.D., 2016. Estimating and projecting the effect of cold waves on mortality in 209 US cities. *Environ. Int.* 94, 141–149.
- Wang, G.Z., Wu, L.Y., Chen, J.B., Song, Y.X., Chen, R.R., 2017. ACEG-based analysis on PM_{2.5}-induced health-related economic effect in Beijing. *China Environ. Sci.* 37, 2779–2785.
- Wang, F., Qiu, X., Cao, J., Peng, L., Zhang, N., Yan, Y., et al., 2020. Policy-driven changes in the health risk of PM_{2.5} and O₃ exposure in China during 2013–2018. *Sci. Total Environ.* 757, 143775 <https://doi.org/10.1016/j.scitotenv.2020.143775> [Internet].
- Wang, S., McGibbon, J., Zhang, Y., 2024. Predicting high-resolution air quality using machine learning: integration of large eddy simulation and urban morphology data. *Environ Pollut* [Internet] 344 (November 2023), 123371. <https://doi.org/10.1016/j.envpol.2024.123371>.
- WHO WHO global air quality guidelines: Particulate matter, 2021. PM_{2.5} and PM₁₀, Ozone, Nitrogen Dioxide, Sulfur Dioxide and Carbon Monoxide. World Health Organization, Geneva.
- Wickham, J., Homer, C., Vogelmann, J., McKerrow, A., Mueller, R., Herold, N., et al., 2014. The multi-resolution land characteristics (MRLC) consortium - 20 years of development and integration of USA national land cover data. *Remote Sens* 6 (8), 7424–7441.
- Wismar, M., Blau, J., Ernst, K.F.J., 2007. The Effectiveness of Health Impact Assessment: Scope and Limitations of Supporting Decision-Making in Europe. WHO Regional Office for Europe, Copenhagen [Internet]. http://www.euro.who.int/_data/assets/pdf_file/0003/98283/E90794.pdf.
- Wondmagegn, B.Y., Xiang, J., Dear, K., Williams, S., Hansen, A., Pisaniello, D., et al., 2021. Increasing impacts of temperature on hospital admissions, length of stay, and related healthcare costs in the context of climate change in Adelaide, South Australia. *Sci. Total Environ.* 773, 145656 <https://doi.org/10.1016/j.scitotenv.2021.145656> [Internet].
- World Bank, 2020. List of Economies [Internet]. https://databankfiles.worldbank.org/public/ddpext_download/site-content/CLASS.xls.
- World Climate Research Programme. Coupled Model Intercomparison Project Phase 5.
- World Health Organisation, 2015. WHO's Source Apportionment Database for PM₁₀ and PM_{2.5} [Internet]. http://www.who.int/quantifying_ehimpacts/global_source_apport/.
- World Health Organisation, 2020. WHO Guidelines on Physical Activity and Sedentary Behaviour. World Health Organization, Geneva.
- World Health Organisation, 2023. Climate Change [Internet]. <https://www.who.int/news-room/fact-sheets/detail/climate-change-and-health>.
- World Health Organisation. World Health Organisation Global Health Estimates 2016: Deaths by Cause, Age, Sex, by Country and by Region, 2000–2016 [Internet]. Available from: <https://www.who.int/data/gho/data/themes/mortality-and-global-health-estimates/ghe-leading-causes-of-death>.
- World Health Organisation. Urban Health Initiative [Internet]. Available from: <https://www.who.int/initiatives/urban-health-initiative>.
- World Health Organization, 2014. WHO Expert Meeting: methods and tools for assessing the health risks of air pollution at local, national and international level. Meeting report 1–112 (May). http://www.euro.who.int/_data/assets/pdf_file/0010/263629/WHO-Expert-Meeting-Methods-and-tools-for-assessing-the-health-risks-of-air-pollution-at-local-national-and-international-level.pdf.
- World Health Organization, 2021. WHO global air quality guidelines: particulate matter (PM_{2.5} and PM₁₀), ozone, nitrogen dioxide, sulfur dioxide and carbon monoxide [Internet]. <https://www.who.int/publications-detail-redirect/9789240034228>.
- World Income Inequality Database [Internet]. Available from: <https://wid.world/>.
- WorldClim, 2020. WorldClim historical climate data [Internet]. <https://www.worldclim.org/data/worldclim21.html>.
- Xiao, Q., Geng, G., Cheng, J., Liang, F., Li, R., Meng, X., et al., 2021a. Evaluation of gap-filling approaches in satellite-based daily PM_{2.5} prediction models. *Atmos Environ* [Internet] 244 (June 2020), 117921. <https://doi.org/10.1016/j.atmosenv.2020.117921>.
- Xiao, Q., Zheng, Y., Geng, G., Chen, C., Huang, X., Che, H., et al., 2021b. Separating emission and meteorological contributions to long-term PM_{2.5} trends over eastern China during 2000–2018. *Atmos. Chem. Phys.* 21 (12), 9475–9496.
- Zanaga, D., Van De Kerchove, R., De Keersmaecker, W., Souverijns, N., Brockmann, C., Quast, R., et al., 2021. ESA WorldCover 10m 2020 v 100 [Internet]. <https://zenodo.org/record/5571936>.
- Zhang, Y., 2021. All-cause mortality risk and attributable deaths associated with long-term exposure to ambient PM_{2.5} in Chinese adults. *Environ. Sci. Technol.* 55 (9), 6116–6127.
- Zhang, Y.L., Cao, F., 2015. Fine particulate matter (PM_{2.5}) in China at a city level. *Sci. Rep.* 5 (2014), 1–12.
- Zhang, M., Song, Y., Cai, X., Zhou, J., 2008. Economic assessment of the health effects related to particulate matter pollution in 111 Chinese cities by using economic burden of disease analysis. *J Environ Manage* 88 (4), 947–954.
- Zhang, X., Cheng, C., Zhao, H., 2022. A health impact and economic loss assessment of O₃ and PM_{2.5} exposure in China from 2015 to 2020. *GeoHealth* 6 (3), 1–15.
- Zheng, P., Barber, R., Sorensen, R.J.D., Murray, C.J.L., Aravkin, A.Y., 2021. Trimmed constrained mixed effects models: formulations and algorithms. *J. Comput. Graph Stat.* 30 (3), 544–556.
- Zhou, M., Wang, H., Zhu, J., Chen, W., Wang, L., Liu, S., et al., 2016. Cause-specific mortality for 240 causes in China during 1990–2013: a systematic subnational analysis for the Global Burden of Disease Study 2013. *Lancet* 387 (10015), 251–272.
- Zhou, B., Rybski, D., Kropp, J.P., 2017. The role of city size and urban form in the surface urban heat island. *Sci. Rep.* 7 (1), 1–9.
- Zhou, M., Wang, H., Zeng, X., Yin, P., Zhu, J., Chen, W., et al., 2019. Mortality, morbidity, and risk factors in China and its provinces, 1990–2017: a systematic analysis for the Global Burden of Disease Study 2017. *Lancet* 394 (10204), 1145–1158. [https://doi.org/10.1016/S0140-6736\(19\)30427-1](https://doi.org/10.1016/S0140-6736(19)30427-1) [Internet].
- Zhu, X.X., Qiu, C., Hu, J., Shi, Y., Wang, Y., Schmitt, M.T.H., 2022. The global urban morphology on our planet - perspectives from space. *Remote Sens. Environ.* 269, 112794.
- Ye, T., Guo, S., Xie, Y., Chen, Z., Abramson, M.J., 2021. Health and related economic benefits associated with reduction in air pollution during COVID-19 outbreak in 367 cities in China. *Ecotoxicol. Environ. Saf.* 222, 112481.